the plant journal

SEB SOCIETY FOR EXPERIMENTAL BIOLOGY

The Plant Journal (2025) **122,** e70145 doi: 10.1111/tpj.70145

Exploring genomic regions and genes modulating plant height and flag leaf morphology in rice

Xianpeng Wang[1,†], Lei Chen[2,†], Zhikun Zhao[1], Ningjia Jiang[3], Najeeb Ullah Khan[1], Qianfeng Hu[1], Ruiqi Liu[1], Zhenkun Liu[3], Xuehan Qian[1], Xiaoyang Zhu[1], Xingming Sun[1,3], Jinjie Li[1,3], Hongliang Zhang[1,3], Danting Li[2], Peng Xu[4], Yinghua Pan[2,*], Zichao Li[1,3,*] and Zhanying Zhang[1,3,*]

[1]*Frontiers Science Center for Molecular Design Breeding, Key Laboratory of Crop Heterosis and Utilization (MOE), Beijing Key Laboratory of Crop Genetic Improvement, College of Agronomy and Biotechnology, China Agricultural University, Beijing 100193, China,*

[2]*Guangxi Key Laboratory of Rice Genetics and Breeding, Rice Research Institute of Guangxi Academy of Agricultural Sciences, Nanning, Guangxi, China,*

[3]*Sanya Institute of China Agricultural University, Sanya, China, and*

[4]*CAS Key Laboratory of Tropical Plant Resources and Sustainable Use, The Xishuangbanna Tropical Botanical Garden, Chinese Academy of Sciences, Menglun, Mengla, Yunnan, China*

Received 17 October 2024; revised 3 March 2025; accepted 26 March 2025.
*For correspondence (e-mail zhangzhanying@cau.edu.cn and lizichao@cau.edu.cn and panyinghua@gxaas.net).
†These authors contributed equally to this work.

SUMMARY

Plant height and flag leaf morphology critically affect plant yield because they determine above-ground plant biomass and photosynthate production. However, few genetic basis analyses and gene mining studies on plant height, flag leaf length, and flag leaf width have been performed, and there is little available information about the evolution and utilization of the underlying natural alleles. This study conducted a genome-wide association study (GWAS) using 689 rice accessions collected from diverse regions across the globe. The GWAS identified 73, 159, and 158 significant loci associated with plant height, flag leaf length, and flag leaf width, respectively. *SD1*^{HAP1} and *NAL1*^{A} were also identified as superior alleles that could be used to improve plant architecture by reducing plant height and increasing flag leaf width, respectively. *LEAF1* and its elite allele *LEAF1*^{G}, which simultaneously modulated plant height and flag leaf morphology, were isolated, and the *LEAF1* knockout lines showed reduced flag leaf length and plant height, whereas *LEAF1*^{G}-complementary lines in the *LEAF1*^{A} background had the opposite phenotypes. The results also showed that *LEAF1*^{G} and *SD1*^{HAP1} evolved directly from wild rice and were mainly found in the *Xian* subgroup, whereas *NAL1*^{A} might have originated from *de novo* mutation during domestication and was mainly found in the *Geng* subgroup. A joint haplotype analysis revealed that pyramiding *SD1*^{HAP1}, *NAL1*^{A}, and *LEAF1*^{G} in Type I accessions optimized plant architecture, reduced plant height, and enlarged the flag leaves. In addition, genomic regions and genes that had been convergently selected for these traits were identified by combining a population genetics analysis with a GWAS. These findings provide valuable genetic targets for molecular breeding that will improve plant height and flag leaf morphology in rice.

Keywords: plant height, flag leaf morphology, GWAS, *LEAF1*, rice.

INTRODUCTION

Plant height and leaf morphology are critical traits when attempting to achieve high rice yields because they influence the formation of above-ground biomass and the provision of sufficient photosynthetic products (Lee et al., 2020; Qu et al., 2017). In the 1960s, the green revolution, which focused on semi-dwarf breeding, considerably increased rice yields by reducing plant height and improving lodging resistance (Liu et al., 2021). However, the reduction in above-ground plant biomass caused by a shorter plant height has led to difficulties when attempting to breed super-high-yield rice varieties. Previous studies on super hybrid rice and ideotype breeding have shown that an appropriate plant height will increase rice yields (Jiao et al., 2010; Zhang, Zhou, et al., 2017). Leaves are the primary source of photosynthate and play a crucial role in the grain filling process. Specifically, flag leaves are the dominant suppliers of photosynthates after flowering and

their length and width determine flag leaf morphology (Acevedo-Siaca et al., 2021; Adachi et al., 2017). Longer and wider flag leaves tend to droop and shield the lower leaves, which reduce the photosynthetic efficiency of the plant. However, shorter and narrower flag leaves will reduce photosynthate production, which will negatively impact yield (He et al., 2018; Rahman et al., 2013). Therefore, an appropriate plant height and flag leaf shape can improve the spatial distribution and the light-receiving ability of the plant, which will increase the light energy and space utilization rate. These improvements should subsequently increase rice yield.

Researchers have cloned a large number of genes that modulate plant height, such as *semi-dwarf 1* (*SD1*) (Sasaki et al., 2002), *gibberellin 20-oxidase 1* (*OsGA20ox1*) (Oikawa et al., 2004), *dwarf-1* (*D1*) (Ueguchi-Tanaka et al., 2000), *dwarf-2* (*D2*) (Hong et al., 2003), *dwarf-35* (*d35*) (Itoh et al., 2004), *dwarf 11* (*d11*) (Tanabe et al., 2005), *xyloglucan endotransglucosylases/hydrolases 8* (*OsXTH8*) (Jan et al., 2004), *GRETCHEN HAGEN3-2* (*OsGH3-2*) (Du et al., 2012), *SEEDLING BIOMASS 1* (*qSBM1*) (Xu et al., 2021), *wall-associated kinases 10* (*OsWAK10*) (Cai et al., 2023) and *exportin 1* (*OsXPO1*) (Peng et al., 2023). The green revolution gene *SD1* encodes gibberellin 20 oxidase-2 (GA20ox2), whereas loss-of-function *SD1* suppresses gibberellin synthesis and internode elongation, which reduces plant height (Sasaki et al., 2002). *OsGH3-2* encodes an indole-3-acetic acid-amido synthetase that modulates free indoleacetic acid (IAA) levels by catalyzing the conjugation of IAA to amino acids. *OsGH3-2* overexpression plants mimic the IAA deficiency phenotype, such as dwarfing and shorter flag leaves (Du et al., 2012).

In contrast, there are only a few genes that use flag leaf width as an index, such as *narrow leaf 1* (*NAL1*) (Qi et al., 2008), *tandem zinc finger protein 1* (*OsTZF1*) (Zhang et al., 2012), *narrow leaf 9* (*NAL9*) (Li et al., 2013), *ovate family protein 1* (*OFP1*) (Xiao et al., 2017), *narrow leaf 8* (*NAL8*) (Chen et al., 2019), *narrow leaf 21* (*NAL21*) (Uzaira et al., 2021), and *wide leaf 1* (*WL1*) (You et al., 2022). *NAL1* encodes for serine/cysteine protease and modulates leaf width by affecting small vein pattern and polar auxin transport (Qi et al., 2008), whereas *NAL21* encodes a ribosomal small subunit protein RPS3A. In *nal21* mutants, decreases in the numbers of free 40s ribosomal subunits, 80s ribosomes, and polysomes affected the protein translation efficiency of several auxin response factors in the 5′-UTR region, which subsequently inhibited auxin-regulated leaf cell division and expansion (Uzaira et al., 2021).

Gene mining for flag leaf length primarily focuses on multiple quantitative trait loci (QTL). In recent years, many QTLs have been mined by linkage mapping (LA) or genome-wide association analyses (GWASs). For example, a total of 295 rice varieties and two recombinant inbred lines (RILs) were used to perform a GWAS and LA, respectively, and detected 36 significant SNPs and 28 QTLs associated with flag leaf size (Wang et al., 2022). Among them, two pleiotropic QTLs, *qFL2/qFWr2-3* and *qFL1/qFWr10*, were identified as potentially containing the candidate genes for flag leaf size. Although several genes modulating plant height and leaf morphology have been cloned, the majority were obtained by reverse genetics or forward genetics approaches using mutant materials. The lack of information about their natural variations in germplasms has restricted the provision of highly valuable genetic resources that could be used to breed varieties with improved morphologies.

Significant morphological variations exist among different rice varieties, particularly between the two major subgroups, *Xian* and *Geng*. They have accumulated abundant genetic variations and have formed their own unique plant morphologies during the long-term evolutionary process. Previous studies revealed that *Xian* varieties have significantly longer and wider flag leaves, thicker and higher culms, longer panicles, and more spikelets per panicle compared with *Geng* varieties (Wang et al., 2023). However, further research is needed to elucidate the primary factors underlying the significant morphological differences among rice subgroups. Additionally, there is a correlation between morphological traits and their genetic basis. Therefore, analyzing the genetic basis of plant height and flag leaf size will provide insights into the phenotypic variations between subgroups at the genome level.

In this study, loci related to plant height and flag leaf morphology were mined using a GWAS based on the variation information retained in rice germplasms. A total of three superior alleles: *SD1*, *NAL1*, and *LEAF1*, were identified, and they modulated plant height, flag leaf width, and flag leaf length, respectively. Pyramiding them could improve plant architecture and grain yield. The genomic regions that simultaneously modulate plant height and leaf morphology were identified and could serve as target loci for molecular design breeding.

RESULTS

Plant height, flag leaf length, and flag leaf width phenotypic variations in rice germplasm

A total of 689 accessions, consisting of 452 *Xian* and 237 *Geng* accessions (200 temperate *Geng* (*TeG*) and 37 tropical *Geng* (*TrG*)) from major rice growing areas of the world, were phenotyped in field trials in 2020 and 2021 to identify the genetic basis of plant height and flag leaf morphology (including leaf length and leaf width) in rice natural germplasm (Figure 1A; Figure S3; Table S1). The observed variations in plant height, flag leaf length, and flag leaf width ranged from 62.9 to 208.8 cm, 15.2 to 57.3 cm, and 0.85 to 2.44 cm, respectively (Figure 1B;

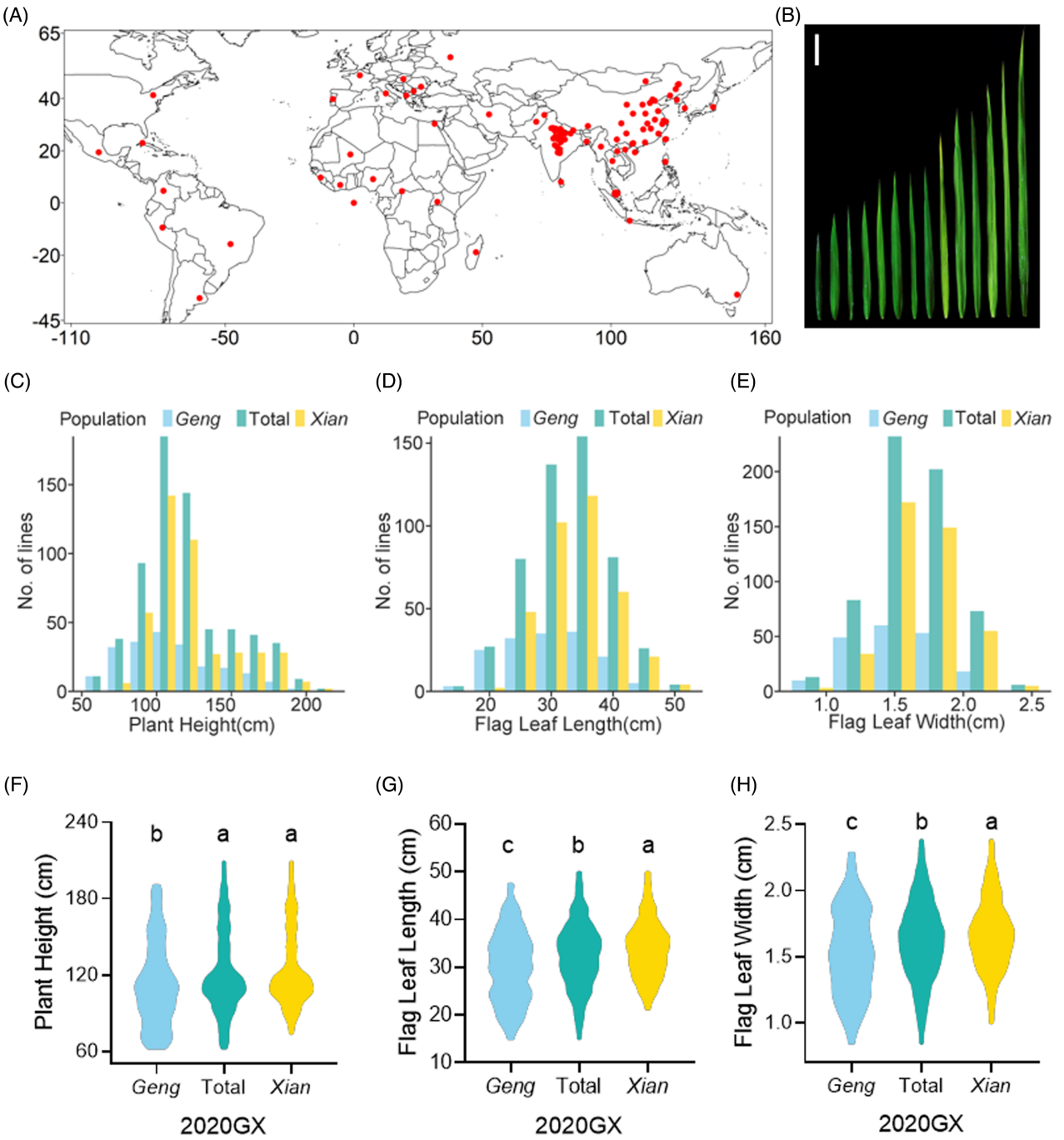

Figure 1. Plant height, flag leaf length, and flag leaf width phenotypic variations in rice germplasm.
(A) Worldwide distribution of the germplasms.
(B) Variations in flag leaf length and flag leaf width. Bars, 4.5 cm.
(C–E) Distribution of the plant height (C), flag leaf length (D) and flag leaf width (E) in the total germplasm, *Xian*, and *Geng* in 2020.
(F–H) Comparison of the plant height (F), flag leaf length (G), and flag leaf width (H) among the total germplasm, *Xian*, and *Geng* in 2020. Data represent means ± SD ($n \geq 157$; $P < 0.05$; one-way ANOVA). The significance for the same lowercase letter is $P \geq 0.05$, while for the different lowercase letters are $P < 0.05$..

Table S2). A statistical phenotype analysis of these three traits showed abundant phenotypic variation and a continuous, positive distribution, indicating that they were modulated by multiple QTLs (Figure 1C–H; Figure S1). In detail, the average plant heights and flag leaf lengths and widths of the *Xian* and *TrG* varieties were significantly greater than those for *TeG* (Figure S2). However, the coefficient of variation for *TeG* was higher than that for *Xian* and *TrG*,

indicating that there may be inter-subspecies and intra-*Geng* genetic differentiation among the three traits (Table S2). In addition, the flag leaf lengths and leaf widths for the 2021 germplasm were greater than those for the 2020 germplasm (Tables S2). Moreover, the positive flag leaf width correlation between the different years was higher than that for flag leaf length, indicating that flag leaf width was more environmentally stable than flag leaf length (Table S3). Meanwhile, plant height was more strongly correlated with flag leaf length than flag leaf width in 2020 and 2021 (Table S3). These results collectively indicated that there were multiple loci modulating plant height, flag leaf length, and flag leaf width.

Genetic basis of the natural variation in plant height, flag leaf length, and flag leaf width revealed by the GWAS

To dissect the genetic basis of these 689 germplasms for plant height and flag leaf length and width, 3 059 978 high-quality nucleotide polymorphisms (SNPs) were filtered out from sequencing data with an average sequencing depth of 15×. The genome-wide linkage disequilibrium (LD) decay of the total germplasm and the *Xian* and *Geng* subspecies ranged from 167.6 to 286 kb, 20.3 to 29 kb, and 236.5 to 357.6 kb, respectively (Figure S4). A GWAS was performed on the total germplasm and the *Xian* and *Geng* subspecies to reveal the genetic basis of the natural variations in plant height, flag leaf length, and flag leaf width. The quantile–quantile plot results led to the adoption of the compressed mixed linear model because it better reduced the level of false positives than the general linear model (Figures S5 and S6). In total, 73, 159, and 158 significant loci associated with plant height, flag leaf length, and flag leaf width were identified, respectively, based on the significance threshold ($P < 0.0001$) calculated by the permutation tests (Figure 2A,B; Table S4; Figures S7–S10). Among them, 39, 29, and 5 significant loci associated with plant height; 43, 11, and 9 significant loci associated with flag leaf length; and 39, 15, and 2 significant loci associated with flag leaf width were identified in the total germplasms and the *Xian* and *Geng* subspecies, respectively, in 2020, whereas 54, 26, and 16 significant loci associated with flag leaf length and 35, 35, and 32 significant loci associated with flag leaf width were identified in the total germplasms and the *Xian* and *Geng* subspecies, respectively, in 2021 (Figure S11A). Furthermore, 11 and 4 loci associated with plant height, 2 and 7 loci associated with flag leaf length, and 2 and 1 loci associated with flag leaf width were consistently detected between the total germplasms and the *Xian* or *Geng* subspecies in 2020 (Figure S11B–D), respectively; 10 and 7 loci associated with flag leaf length and 6 and 7 loci associated with flag leaf width were consistently detected between the total germplasms and the *Xian* or *Geng* subspecies in 2021 (Figure S11E,F), respectively, and 8 and 15 loci associated with flag leaf length and flag leaf width were consistently detected between 2020 and 2021, respectively (Figure S11G,H). The 13 loci associated with both plant height and flag leaf length, the 3 loci associated with plant height and flag leaf width, and the 7 loci associated with flag leaf length and flag leaf width suggested that these loci synergistically modulated these traits (Figure 2C).

Determination of the *SD1* and *NAL1* superior alleles

The genes in highly significant loci that were consistently detected across different populations or different traits were screened to isolate the reliable loci conferring these traits. For instance, the "Green Revolution" gene *SD1* was found in a significant plant height locus called *qPH1.14/qPH1.22* that was found in both the total germplasms and the *Xian* subspecies (Figure 3A,B; Table S4). The loss-of-function *SD1* led to reduced plant height and enhanced lodging resistance, which are characteristics that have been widely used to increase rice yield (Liu et al., 2021). The accessions were divided into four major haplotypes based on the significant SNPs in the promoter region and the significant non-synonymous SNPs in the coding region and were named HAP1–HAP4 (Figure 3C,D). There were four haplotypes in the *Xian* subgroup, and the accessions containing HAP1 had significantly lower plant heights than the accessions containing the other three haplotypes. There were two haplotypes (HAP1 and HAP2) in the *Geng* subgroup, and the plant heights of the accessions containing HAP2 were slightly greater than the accessions containing HAP1 (Figure 3E,F). These results implied that $SD1^{HAP1}$ was the superior allele and could improve plant architecture by reducing plant height.

Another significant locus for flag leaf width, *qFLW4.3/qFLW4.5*, was also consistently detected in the total and the *Xian* germplasms and contained the flag leaf width gene *NAL1* (Figure 3G,H; Table S4). The accessions could be divided into five haplotypes, namely, HAP1–HAP5, based on the variations in the *NAL1* promoter and coding regions. HAP1 was mainly found in *Xian*, and HAP2 was mainly found in *Geng* (Figure 3I,J). The accessions containing HAP2 had wider leaves than the accessions containing the other haplotypes (Figure S12A,B). In addition, only one significant non-synonymous SNP (31 212 801, G to A, Arg to His), located on the third exon, was isolated (Figure 3I,J). The *Xian* and *Geng* accessions with SNP-31212801-A in HAP2 had significantly wider leaves than those with SNP-31212801-G (Figure 3K,L). These results indicated that NAL^{A} was the superior allele and could improve yield by increasing the flag leaf width.

Identification of *LEAF1* modulating flag leaf length

In addition to the cloned genes mentioned above, one significant locus for flag leaf length, *qFLL8.1/qFLL8.6* on chromosome 8, was consistently detected in the total and the

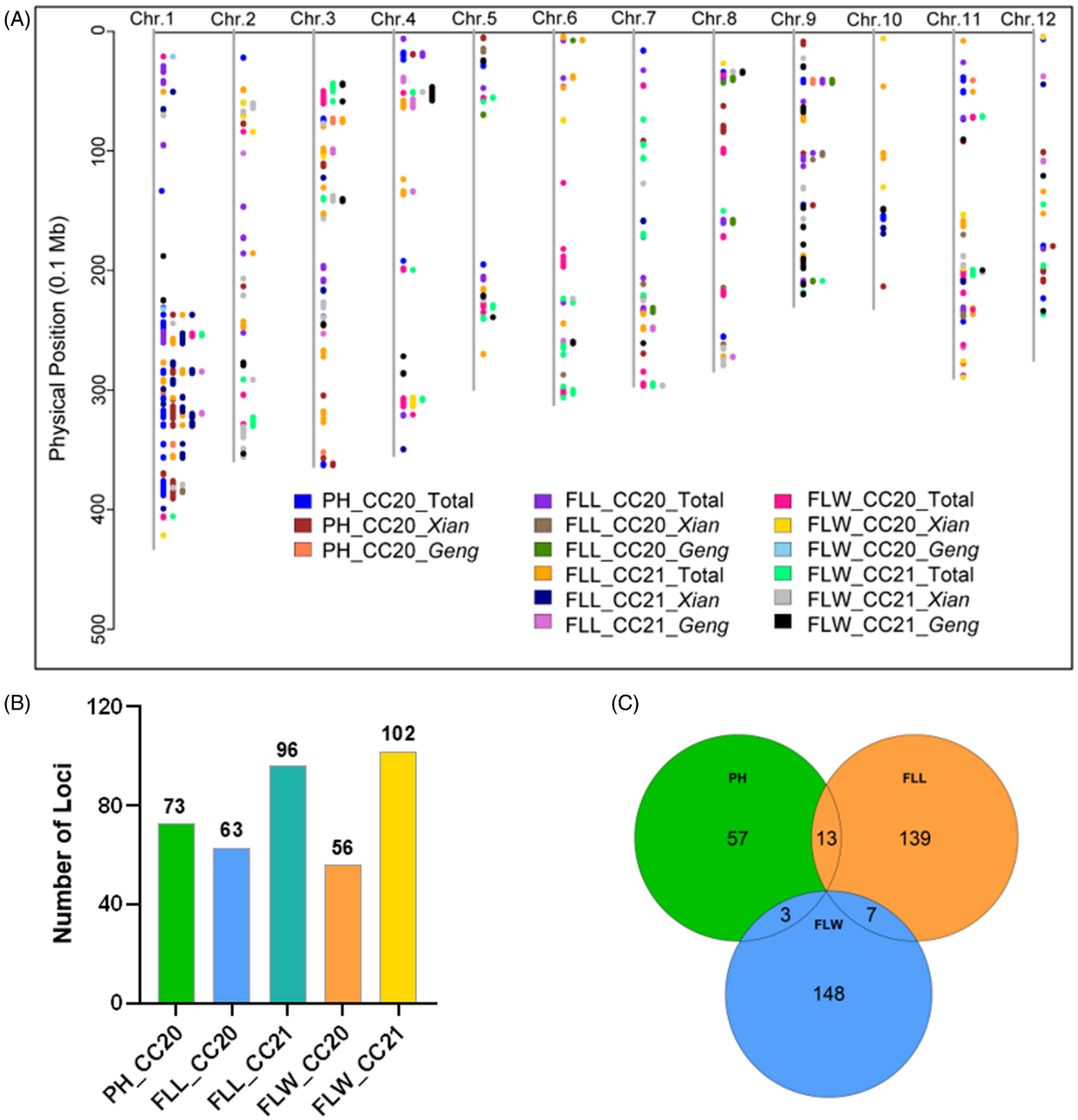

Figure 2. Genetic basis of the natural variation in plant height, flag leaf length, and flag leaf width revealed by the GWAS.
(A) Distribution of the identified loci related to plant height, flag leaf length, and flag leaf width in 12 chromosomes.
(B) Number of loci identified in the total germplasm, *Xian*, and *Geng* for the years 2020 and 2021, respectively.
(C) Venn plot of co-loci across the plant height, flag leaf length, and flag leaf width. PH_CC20_Total, the plant height of the total germplasm in 2020; PH_CC20_*Xian*, the plant height of *Xian* in 2020; PH_CC20_*Geng*, the plant height of *Geng* in 2020. FLL_CC20_Total, the flag leaf length of the total germplasm in 2020; FLL_CC20_*Xian*, the flag leaf length of *Xian* in 2020; FLL_CC20_*Geng*, the flag leaf length of *Geng* in 2020; FLL_CC21_Total, the flag leaf length of the total germplasm in 2021; FLL_CC21_*Xian*, the flag leaf length of *Xian* in 2021; FLL_CC21_*Geng*, the flag leaf length of *Geng* in 2021. FLW_CC20_Total, the flag leaf width of the total germplasm in 2020; FLW_CC20_*Xian*, the flag leaf width of *Xian* in 2020; FLW_CC20_*Geng*, the flag leaf width of *Geng* in 2020; FLW_CC21_Total, the flag leaf width of the total germplasm in 2021; FLW_CC21_*Xian*, the flag leaf width of *Xian* in 2021; FLW_CC21_*Geng*, the flag leaf width of *Geng* in 2021.

Geng germplasms (Figure 4A,B; Table S4). A local LD analysis was performed to determine the underlying candidate genes, and the results showed that *qFLL8.1* had been narrowed down to a 160 kb LD block at the 3.89–4.05 Mb position where the significant SNPs were distributed in the promoter or coding region of 10 genes. Therefore, these genes were selected as potential candidate genes for further analysis (Figure 4C; Figure S13A). The haplotypes of

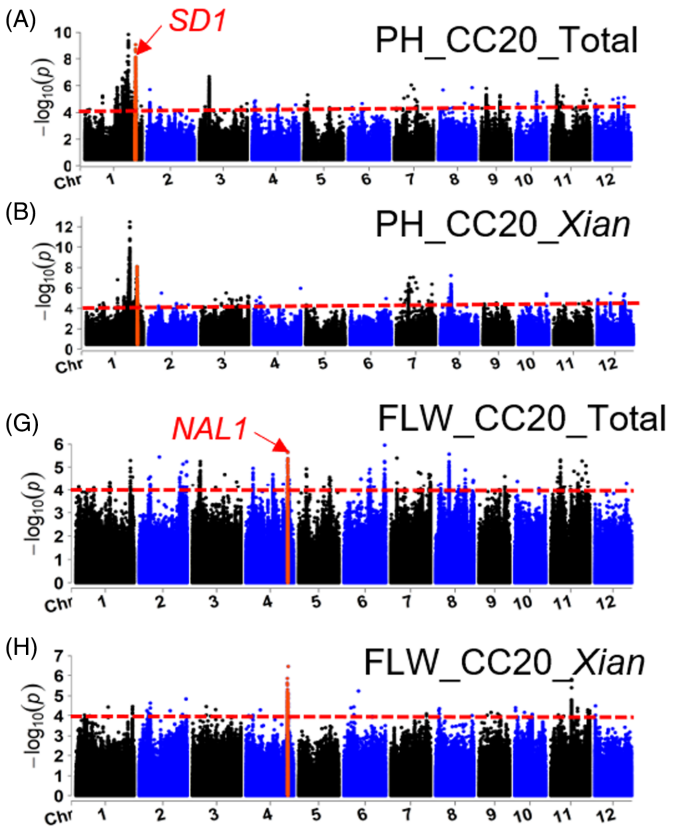

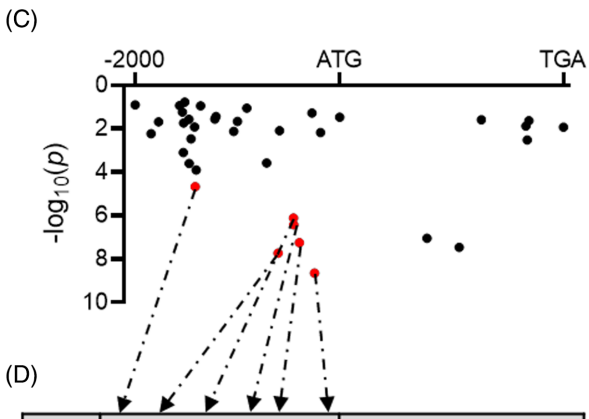

(D)

HAP.	Promoter						No.			
	38380986	38381785	38381934	38381935	38381991	38382137	*Xian*	*Geng*	*TeG*	*TrG*
HAP1	A	T	T	A	T	A	365	17	16	1
HAP2	G	C	G	G	C	G	29	160	132	28
HAP3	A	C	G	G	C	G	15	0	0	0
HAP4	A	T	T	A	C	G	5	0	0	0

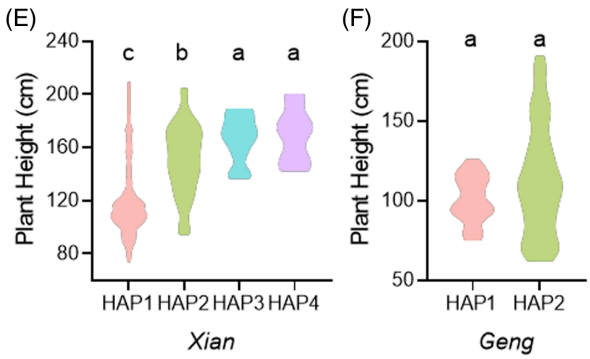

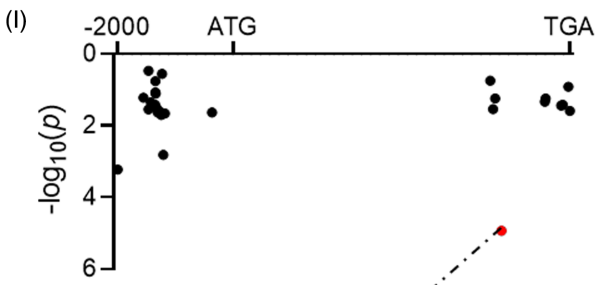

(J)

HAP.	Promoter							CDS			No.			
	31202015	31202739	31202885	31202949	31203234	31203246	31203300	31212801	31214019	31214045	*Xian*	*Geng*	*TeG*	*TrG*
HAP1	G	C	T	A	C	C	T	G	C	G	223	0	0	0
HAP2	G	A	G	G	T	T	T	A	T	A	12	106	85	21
HAP3	G	A	G	G	T	T	T	G	T	A	55	33	33	0
HAP4	A	C	T	A	C	C	A	G	C	G	24	0	0	0
HAP5	G	C	G	G	C	T	T	G	C	G	25	0	0	0

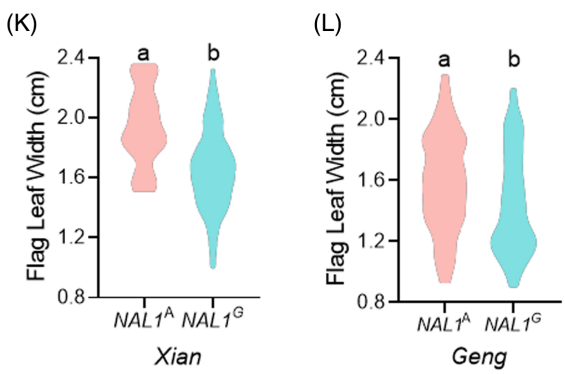

Figure 3. Determination of the *SD1* and *NAL1* superior alleles.
(A, B) Manhattan plots of GWAS for the total germplasm (A) and *Xian* (B) in 2020. Red dots indicate loci containing cloned gene *SD1*.
(C) Local plot of *SD1*. Red dots are significant SNPs within *SD1*.
(D) Haplotype analysis based on the significant SNPs in the promoter region of *SD1*.
(E, F) The plant height among haplotypes of *SD1* in *Xian* (E) *and Geng* (F). Data represent means ± SD ($n \geq 5$; $P < 0.05$; one-way ANOVA). The significance for the same lowercase letter is $P \geq 0.05$, while for the different lowercase letters are $P < 0.05$.
(G, H) Manhattan plots of GWAS in the total germplasm (G) and *Xian* (F) in 2020. Red dots contain cloned gene *NAL1*.
(I) Local plot of *NAL1*. Red dots are significant SNPs within *NAL1*.
(J) Haplotype analysis based on SNPs in the promoter and coding region of *NAL1*.
(K, L) The flag leaf width between germplasms containing $NAL1^{A}$ and $NAL1^{G}$ in *Xian* (K) and *Geng* (L). Data represent means ± SD ($n \geq 15$; $P < 0.05$; one-way ANOVA). The significance for the same lowercase letter is $P \geq 0.05$, while for the different lowercase letters are $P < 0.05$.

these genes were analyzed, and the qRT-PCR results showed that there were no significant differences in their expression levels among the different haplotype varieties (Figures S13B–J and S14A; Table S5). However, only *LOC_Os08g07010*, *LOC_Os08g07030*, and *LOC_Os08g07040* contained significant non-synonymous SNPs in their functional encoding regions (Figure S13A). *LOC_Os08g07010* was predicted to encode an ABC-2 transporter protein, whereas *LOC_Os08g07030* and *LOC_Os08g07040* were predicted to encode proteins with unknown functions. A tissue expression analysis based on the RiceXpro database revealed that *LOC_Os08g07010* expression was greatest in the leaves, roots, and stems (Figure S14B). In addition, *AtABCG14*, the closest orthologous gene to *LOC_Os08g07010* in *Arabidopsis* (Figure S14C), was mainly responsible for transporting cytokinins from the roots to the leaves. Notably, loss-of-function mutants of *AtABCG14* displayed reduced rosette leaf size (Ko et al., 2014). Therefore, *LOC_Os08g07010* was considered the most likely candidate gene for *qFLL8.1* and was named *LONGER FLAG LEAF1* (*LEAF1*).

A total of five major *LEAF1* haplotypes, namely, HAP1–HAP5, were identified based on 21 SNPs in the promoter region and the non-synonymous SNPs in the coding region (Figure 4D). The *Xian* accessions containing HAP1, HAP2, and HAP3 had similar flag leaf lengths, whereas the *Geng* accessions containing HAP1 had a significantly longer flag leaf than the accessions containing HAP4 and HAP5 (Figure 4E,F). Moreover, a local LD analysis of *LEAF1* showed that the linkage degree in the coding region was greater than that in the promoter region. Two significant SNPs (SNP-3928812, G to A, Gly to Ser and SNP-3932102, G to A, Gly to Ser) were located in the coding region. SNP-3928812 was the leader SNP and was located at the 350th base downstream of the initiation codon for *LEAF1* (Figure S15A). Additionally, the frequencies of the major and minor alleles at each SNP in the different haplotypes revealed that SNP-3928812 was the major allele in the long flag leaf haplotypes (HAP1, HAP2, and HAP3) and the minor allele in the short flag leaf haplotypes (HAP4 and HAP5). The accessions with SNP-3928812-G had a significantly longer flag leaf than those with SNP-3928812-A (Figure 4G; Figure S15B). Taken together, these results suggested that *LEAF1* could be the causal gene for *qFLL8.1*.

The function of *LEAF1* was assessed using a CRISPR/Cas9-mediated approach to generate knockout mutants in the "Hexi 41" background (HAP1). This method effectively generated two independent frameshift mutant lines, namely, *leaf1*-1 and *leaf1*-2, respectively (Figure S16A). The *leaf1*-1 and *leaf1*-2 flag leaf lengths were significantly shorter than those of the wild-type (WT) plants (Figure 4J). In addition, the effects of *LEAF1* on other important agronomic traits were investigated and the results showed that *leaf1*-1 and *leaf1*-2 plants had lower plant heights, narrower flag leaf widths, thinner stems, shorter panicle lengths, decreased primary and secondary branches and reduced grain numbers compared with WT, which resulted in the decreased sink capacity and grain yields, although the grain lengths, grain widths, and 1000-grain weights significantly increased (Figure 4J; Figure S16B–O). Furthermore, the accessions with SNP-3928812-G were significantly taller than those with SNP-3928812-A (Figure S17). Subsequently, we complemented the $LEAF1^{G}$ allele from the "Huanghuazhan" (HAP1) accession into the "ZhongHua 11" (HAP4) background. Phenotypic analysis revealed a significant increase in flag leaf length in *LEAF1*-Com plants compared with the "ZhongHua 11" control ("ZH11") (Figure S18). These results implied that *LEAF1* was a pleiotropic gene that played a critical role in rice development and that $LEAF1^{G}$ could be a superior allele that confers a longer flag leaf.

Evolution and utilization of *LEAF1* in breeding

A haplotype network was constructed for 76 wild rice and 471 cultivated rice accessions to investigate the *LEAF1* origin and evolution process during rice domestication. The results showed that most *Xian*, *TrG*, and *TeG* accessions that contained the $LEAF1^{G}$ allele with longer flag leaves (*Xian*-FLL-L, *TrG*-FLL-L, and *TeG*-FLL-L) had directly evolved from wild rice. Among them, *Xian*-FLL-L had mainly evolved from *Oryza nivara* 2 (*Niv2*) and *Oryza rufipogon* 2 (*Ruf2*) and *TrG*-FLL-L and *TeG*-FLL-L had evolved from *O. rufipogon* 1 (*Ruf1*). The $LEAF1^{A}$ allele had directly evolved from *Ruf1* wild rice and was specifically preserved in *Xian* and *TeG* accessions with short flag leaves (*Xian*-

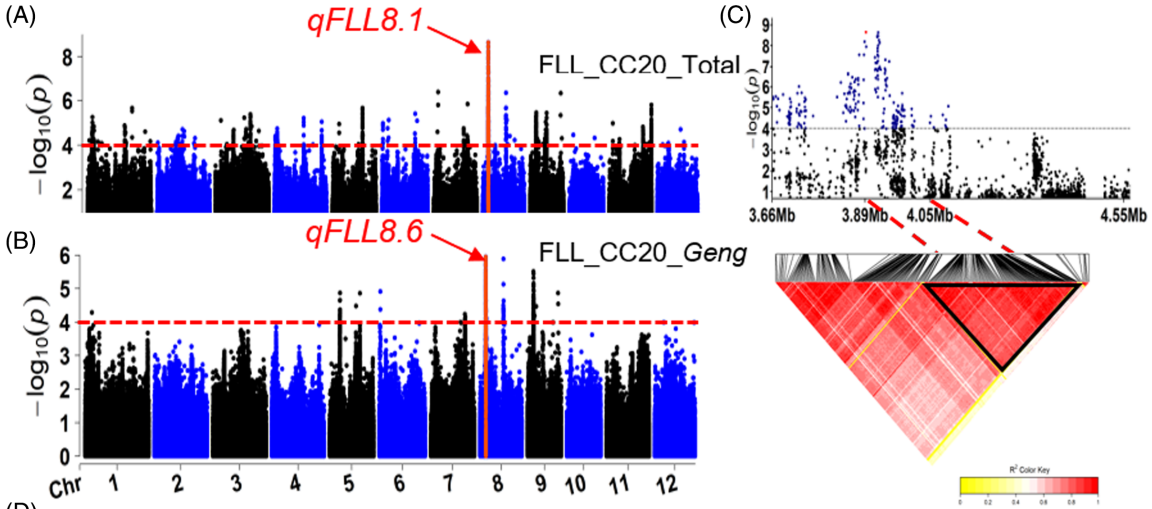

(D)

HAP	Promoter													CDS							No.			
	3926528	3926602	3926771	3926870	3927070	3927158	3927166	3927167	3927171	3927724	3927865	3928010	3928071	3928221	3928783	3928806	3928812	3928993	3929014	3929017	3932102	*Xian*	*Geng*	*TeG*	*TrG*
HAP1	A	C	C	A	A	A	T	A	A	C	A	G	A	C	G	G	G	A	A	A	G	117	60	42	18
HAP2	G	G	A	G	G	G	A	G	G	G	T	A	C	A	A	T	G	C	G	G	G	62	0	0	0
HAP3	G	G	A	G	G	G	A	G	G	G	T	A	C	A	G	T	G	C	G	G	G	127	0	0	0
HAP4	G	C	C	G	G	A	T	G	G	C	A	G	A	C	G	G	A	A	A	A	A	0	54	54	0
HAP5	G	C	C	G	G	A	T	G	G	C	A	G	A	C	G	G	A	A	A	A	G	0	11	11	0

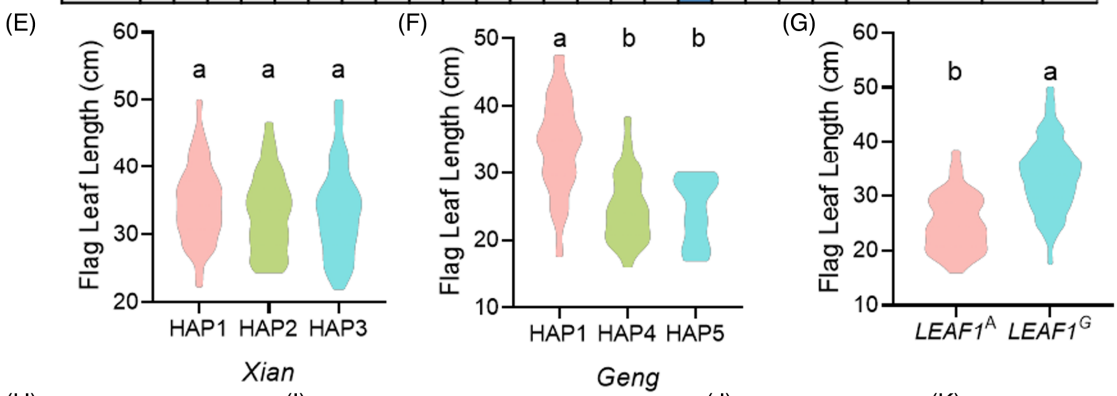

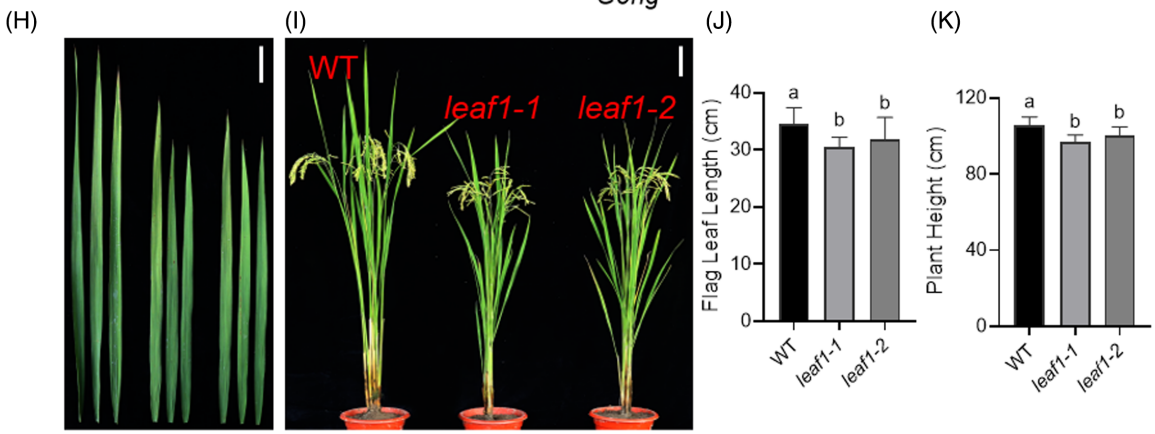

Figure 4. Identification of *LEAF1* modulating flag leaf length.
(A, B) Manhattan plots of GWAS in the total germplasm (A) and *Geng* (B) in 2020. Red dots represent *qFLL8.1/qFLL8.6* loci.
(C) Local manhattan plots and LD heatmap. Black inverted triangle represents an LD block region containing the Lead-SNP of *qFLL8.1*.
(D) Haplotype analysis based on the SNPs in the promoter region and the non-synonymous SNPs in the coding region of *LEAF1*.
(E, F) The flag leaf length among haplotypes of *LEAF1* in *Xian* (E) *and Geng* (F). Data represent means ± SD ($n \geq 10$; $P < 0.05$; one-way ANOVA). The significance for the same lowercase letter is $P \geq 0.05$, while for the different lowercase letters are $P < 0.05$.
(G) Comparison of flag leaf length between germplasms containing $LEAF1^{A}$ and $LEAF1^{G}$. Data represent means ± SD ($n \geq 67$; $P < 0.05$; one-way ANOVA). The significance for the same lowercase letter is $P \geq 0.05$, while for the different lowercase letters are $P < 0.05$.
(H, I) Flag leaf (H) and plant (I) morphology of WT, *leaf1*-1, and *leaf1*-2. Bars, 3.5 cm (H) and 10 cm (I).
(J, K) The flag leaf length (J) and plant height (K) of WT, *leaf1*-1, and *leaf1*-2. Data represent means ± SD ($n \geq 10$; $P < 0.05$; one-way ANOVA). The significance for the same lowercase letter is $P \geq 0.05$, while for the different lowercase letters are $P < 0.05$.

FLL-S, *TeG*-FLL-S) (Figure 5A). The nucleotide diversity and Tajima's *D* value for *LEAF1* and its 100 kb flanking regions were calculated to determine whether *LEAF1* was selected during evolution. On average, the *LEAF1* nucleotide diversity in *Xian* was higher ($\pi = 0.00238$) than in *Geng* ($\pi = 0.00153$) and in *TrG* ($\pi = 0.00046$) and *TeG* ($\pi = 0.00158$). When the *Geng* accessions were further divided into *Geng-LEAF1*^{A} and *Geng-LEAF1*^{G}, the π value for *Geng-LEAF1*^{A} ($\pi = 0.00015$) was much lower than that for *Geng-LEAF1*^{G} ($\pi = 0.00095$). Tajima's *D* value was significantly positive for *LEAF1* in *Xian* (Tajima's $D = 4.334$), but was significantly negative in *TrG* (Tajima's $D = -1.896$) and *Geng-LEAF1*^{A} (Tajima's $D = -1.998$) (Figure 5B,C; Table S6). Taken together, these results indicated that balancing selection for *LEAF1* occurred in *Xian*, whereas positive selection for *LEAF1*^{G} occurred in *TrG* and for *LEAF1*^{A} occurred in *TeG*.

The *LEAF1*^{G} and *LEAF1*^{A} allele frequencies in the improved varieties (IMPs) and landraces (LANs) were analyzed to investigate their potential utilization in breeding. The results showed that the *LEAF1*^{G} frequency was much higher in both the IMPs and LANs of *Xian* and *TrG* than that of *TeG* accessions, while the *LEAF1*^{A} frequency was slightly higher in the *TeG* IMPs compared with the LANs (Figure 5D). The flag leaf lengths and widths of the IMPs containing the *Geng-LEAF1*^{G} allele increased from 26.7 to 35.3 cm and from 1.3 to 1.74 cm, respectively, compared with the LANs containing the *Geng-LEAF1*^{A} allele (Table S7). The introgression line (IL) IL81 was also isolated. It contained segments from *TrG* accession IRAT109 with the *LEAF1*^{G} allele in the background of the *TeG* accession Yuefu, which contained the *LEAF1*^{A} allele. The IL81 flag leaf lengths and plant heights were significantly greater than those for the Yuefu plants (Figure 5E–H), which suggested that the *LEAF1*^{G} allele could be used to increase flag leaf length and improve the leaf architecture of *TeG* accessions.

Pyramiding of *SD1*, *NAL1*, and *LEAF1* improves plant architecture and grain yield

Haplotype networks for *SD1* and *NAL1* were constructed and the results showed that *SD1*^{HAP1} directly evolved from *Niv2* and was selectively preserved in most *Xian* varieties with relatively low plant heights (*Xian*-PH-L) (Figure S19A). Furthermore, *NAL1*^{G} directly evolved from different wild rice types and was preserved in the *TeG* and most *Xian* accessions, whereas *NAL1*^{A} was derived from a *de novo* mutation (Figure S20A). Moreover, the frequency of the *SD1*^{HAP1} allele increased in IMP varieties compared with the LANs. However, it could potentially be utilized in *Geng* (Figure S19B). Furthermore, the frequency of the *NAL1*^{A} allele significantly increased in the *Geng* IMPs compared with the LANs (Figure S20B). A joint haplotype analysis of *SD1*, *NAL1*, and *LEAF1* was performed and the results showed that there were three main *Xian* types and four main *Geng* types (Figure 6A). Among them, *Xian* types II/III and *Geng* type III directly evolved from wild rice, while *Xian* type I and *Geng* types I/IV/V went through an additional *NAL1*^{G} to *NAL1*^{A} mutation process (Figure 6B). Type I was an aggregation of three elite alleles, namely, *SD1*^{HAP1}, *NAL1*,^{A} and *LEAF1*^{G}. The accessions harboring Type I had significantly reduced plant heights and longer and wider flag leaves (Figure 6E,F). In addition, an agronomic traits analysis of Type I showed that the average plant heights, flag leaf lengths, flag leaf widths, grain numbers, tiller numbers, and 1000-grain weights were 115.8 cm, 36.4 cm, 2.04 cm, 239, 10.4, and 24.1 g for *Xian* and 101.4 cm, 32.6 cm, 1.77 cm, 179, 9.1, and 23.9 g for *Geng*, respectively (Figure 6I–N). Therefore, pyramiding *SD1*^{HAP1}, *NAL1*,^{A} and *LEAF1*^{G} provides abundant genetic resources and a preliminary reference for breeding ideal plant heights and flag leaf morphologies.

Uncovering genomic regions simultaneously modulating plant height and leaf morphology

The *Xian* and *TrG* accessions were taller and had longer and wider flag leaves than the *TeG* accessions. Furthermore, the intra-*TeG* variations for these three traits were larger than those for the *Xian* and *TrG* accessions (Figure S2; Table S2). The differences in the genetic basis underlying the variations in plant height and flag leaf morphology for the different subspecies were investigated by selecting 136, 160, and 150 *Xian* accessions; 16, 20, and 20 *TrG* accessions; and 47, 30, and 40 *TeG* accessions with high plant heights (PH-H), long flag leaf lengths (FLL-L) or wide flag leaf widths (FLW-W). These were then compared with 65, 50, and 70 *TeG* accessions with low plant heights

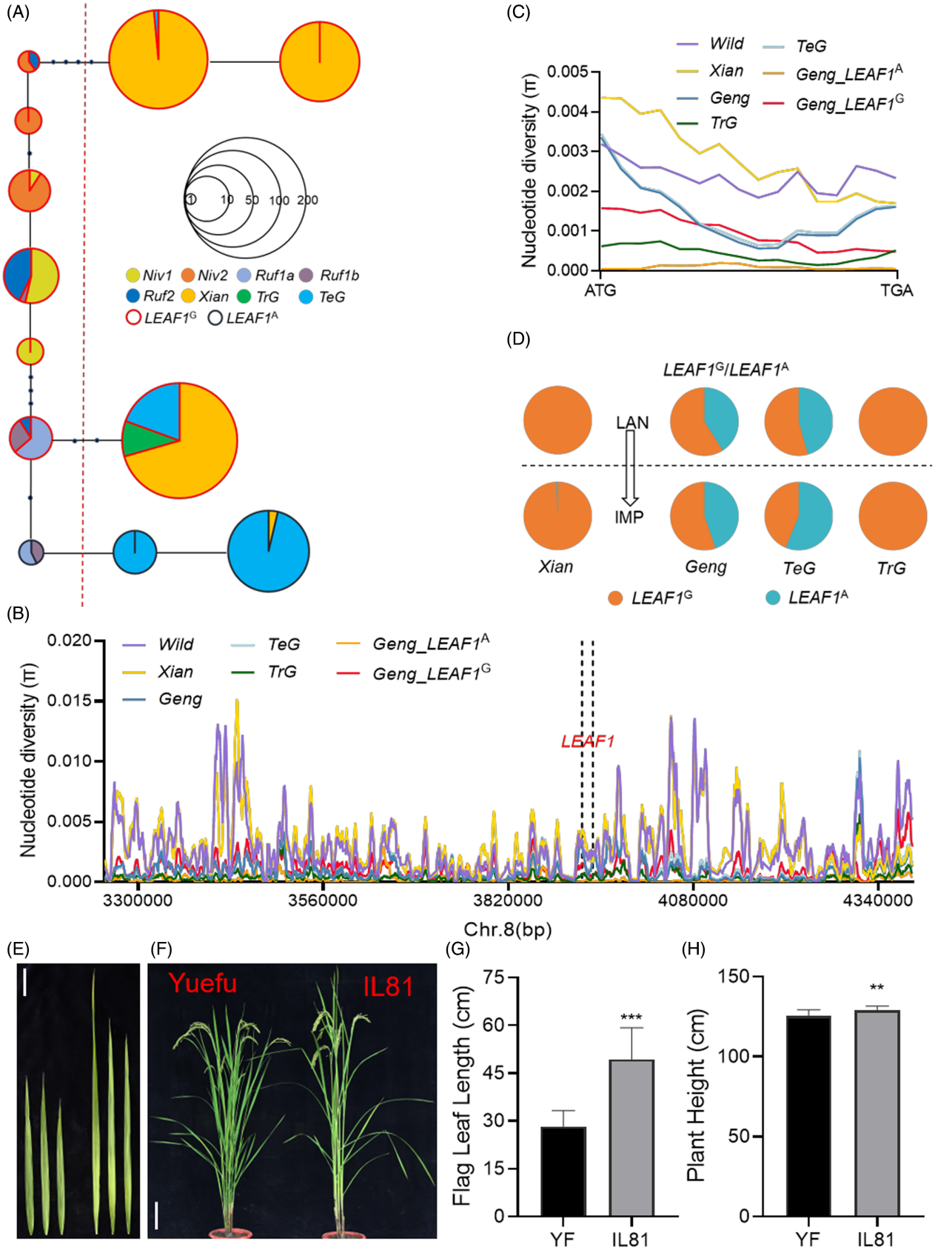

Figure 5. Evolution and utilization of *LEAF1* in breeding.
(A) Evolution relationship of *LEAF1* revealed by a combined minimum spanning tree. *TeG*, temperate *Geng*; *TrG*, tropical *Geng*; *Niv 1/2*, *Oryza nivara 1/2*; *Ruf 1a/1b/2*, *Oryza rufipogon 1a/1b/2*. Red blank circle represents $LEAF1^{G}$ allele and black blank circle represents $LEAF1^{A}$ allele.
(B) The nucleotide diversity of *LEAF1* and its flanking regions.
(C) The local nucleotide diversity of *LEAF1*.
(D) Allelic changes in *LEAF1* during rice breeding. LAN, landraces; IMP, improved varieties.
(E, F) Flag leaf (E) and plant (F) morphology of Yuefu and IL81. Bars, 5 cm (E) and 13.5 cm (F).
(G, H) The flag leaf length and plant height of Yuefu and IL81. Data represent means ± SD ($n \geq 15$; $^{**}P < 0.01$, $^{***}P < 0.001$; Student's *t*-test).

(PH-L), short flag leaf lengths (FLL-S) or narrow flag leaf widths (FLW-N) (Table S1). The genetic differentiated regions in them were then analyzed by calculating population differentiation statistics (F_{ST}). A total of 111, 96, and 117 genomic regions for plant height (Figures S21A, S22A and S23A; Tables S8–S10); 105, 94, and 62 genomic regions for flag leaf length (Figures S21B, S22B and S23B; Tables S11–S13) and 108, 83, and 62 genomic regions for flag leaf width (Figures S21C, S22C, and S23C; Tables S14–S16) were found to be highly divergent between *Xian* and *TeG*, *TrG* and *TeG*, and intra-*TeG*, respectively. These regions were then compared with the QTLs regions isolated by the GWAS, and 6, 7, and 11 overlapping regions for plant height (Figure 7A; Table S17); 15, 11, and 17 overlapping regions for flag leaf length (Figure 7B; Table S18) and 16, 12, and 9 overlapping regions for flag leaf width (Figure 7C; Table S19) were identified between *Xian* and *TeG*, *TrG* and *TeG*, and intra-*TeG*, respectively.

The nucleotide diversity (π) and Tajima's *D* value were calculated to explore whether these regions had been selected. The results showed that the π value for *TeG* with shorter plant heights (*TeG*-PH-L) was lower than that for the *TrG* and *TeG* with higher plant heights (*TrG*-PH-H and *TeG*-PH-H), but was larger than that for *Xian* with higher plant heights (*Xian*-PH-H) (Figure S24A–C; Table S17). Tajima's *D* analysis consistently showed that *Xian*-PH-H and *TeG*-PH-L were under directional selection, but most genetic regions were under neutral evolution in *TeG*-PH-H (Table S17). Moreover, the π value for *TeG* with shorter flag leaf lengths (*TeG*-FLL-S) was lower than that of *TrG*, *TeG*, or *Xian* with longer flag leaves (*TrG*-FLL-L, *TeG*-FLL-L and *Xian*-FLL-L) (Figure S24D–F; Table S18). The Tajima's *D* analysis also showed that most genetic regions were under directional selection in *TeG*-FLL-S, most were under balancing selection in *TeG*-FLL-L and most were under neutral selection in *Xian*-FLL-L and *TrG*-FLL-L (Table S18). Similarly, the π values for *TeG* with narrow flag leaf widths (*TeG*-FLW-N) were lower than those *TrG*, *TeG*, or *Xian* with wider flag leaf widths (*TrG*-FLW-W, *TeG*-FLW-W and *Xian*-FLW-W) (Figure S24G–I; Table S19). In addition, the Tajima's *D* analysis showed that most genetic regions were under directional selection in *TeG*-FLW-N and *Xian*-FLW-W, most were under balancing selection in *TeG*-FLL-W, and most were under neutral selection in *TrG*-FLL-W (Table S19).

There were 71.17% (about 23.24 Mb), 70.27% (about 22.86 Mb), and 75.24% (about 25.69 Mb) overlapping divergent regions between *Xian* and *TeG* for plant height and flag leaf length, plant height and flag leaf width, or flag leaf length and width, respectively, and 59.46% (about 19.89 Mb) had overlapping divergent regions across all three traits (Figure 7D; Table S20). Similarly, there were 66.67% (about 22.49 Mb), 52.08% (about 17.71 Mb) and 64.89% (about 21.07 Mb) overlapping divergent regions between *TrG* and *TeG* for plant height and flag leaf length, plant height and flag leaf width, or flag leaf length and width, respectively, and 45.83% (about 16.42 Mb) had overlapping divergent regions across all three traits (Figure 7D; Table S20). There were 27.35% (about 9.36 Mb), 4.27% (about 1.15 Mb) and 16.13% (about 4.84 Mb) overlapping divergent regions intra-*TeG* for plant height and flag leaf length, plant height and flag leaf width, or flag leaf length and width, respectively, and 2.56% (about 0.55 Mb) had overlapping divergent regions across all three traits (Figure 7D; Table S20). Among these regions, *OsGH3-2* was identified as being in the GWAS *qPH1.10*/*qFLL1.33* QTL, and there were divergent regions between *TeG*-PH-L and *TrG*-PH-H, and *TeG*-FLL-S and *TrG*-FLL-L (Figure 7E; Figure S22A,B), which has been reported to modulate plant height and leaf development in rice (Du et al., 2012). *LEAF1* was identified as being in the GWAS *qFLL8.1* QTL, and there were divergent regions between *TeG*-PH-L and *TeG*-PH-H, and *TeG*-FLL-S and *TeG*-FLL-L (Figure 7F; Figure S23A,B). *OsGH3-2* nucleotide diversity was lower in *TeG*-PH-L and *TeG*-FLL-S than in *TrG*-PH-H and *TrG*-FLL-L (Figure 7G) and *LEAF1* nucleotide diversity was lower in *TeG*-PH-L and *TeG*-FLL-S than in *TeG*-PH-H and *TeG*-FLL-L (Figure 7H), indicating that *OsGH3-2* and *LEAF1* might have undergone convergent selection for lower plant height and shorter flag leaves during rice domestication. Together, these results implied that these traits contained reliable pleiotropic genomic regions.

DISCUSSION

The GWAS identified 73, 159, and 158 significant loci associated with plant height, flag leaf length, and flag leaf width, respectively. *LEAF1*, modulating flag leaf length, and the elite alleles *SD1* and *NAL1* were also identified in the natural germplasm. The superior alleles $LEAF1^{G}$ and $SD1^{HAP1}$ evolved directly from wild rice and were utilized in *Xian*, while $NAL1^{A}$ might be from *de novo* mutation and was utilized in *Geng* during the breeding process.

(A)

Groups	Sub-species	*SD1*^{HAP1}	*NAL1*^{A}	*LEAF1*^{G}	No.	PH (cm)	FLL (cm)	FLW (cm)
I	*Xian*	+	+	+	11	115.8b	36.4ab	2.04a
II		+	-	+	248	115.9b	33.1b	1.66b
III		-	-	+	29	157.6a	37.5a	1.59b
I	*Geng*	+	+	+	13	101.4b	32.6b	1.77a
IV		-	+	+	23	125.4a	37a	1.79a
V		-	+	-	42	85.6c	23.8c	1.45b
III		-	-	+	19	130.7a	30.7b	1.45b

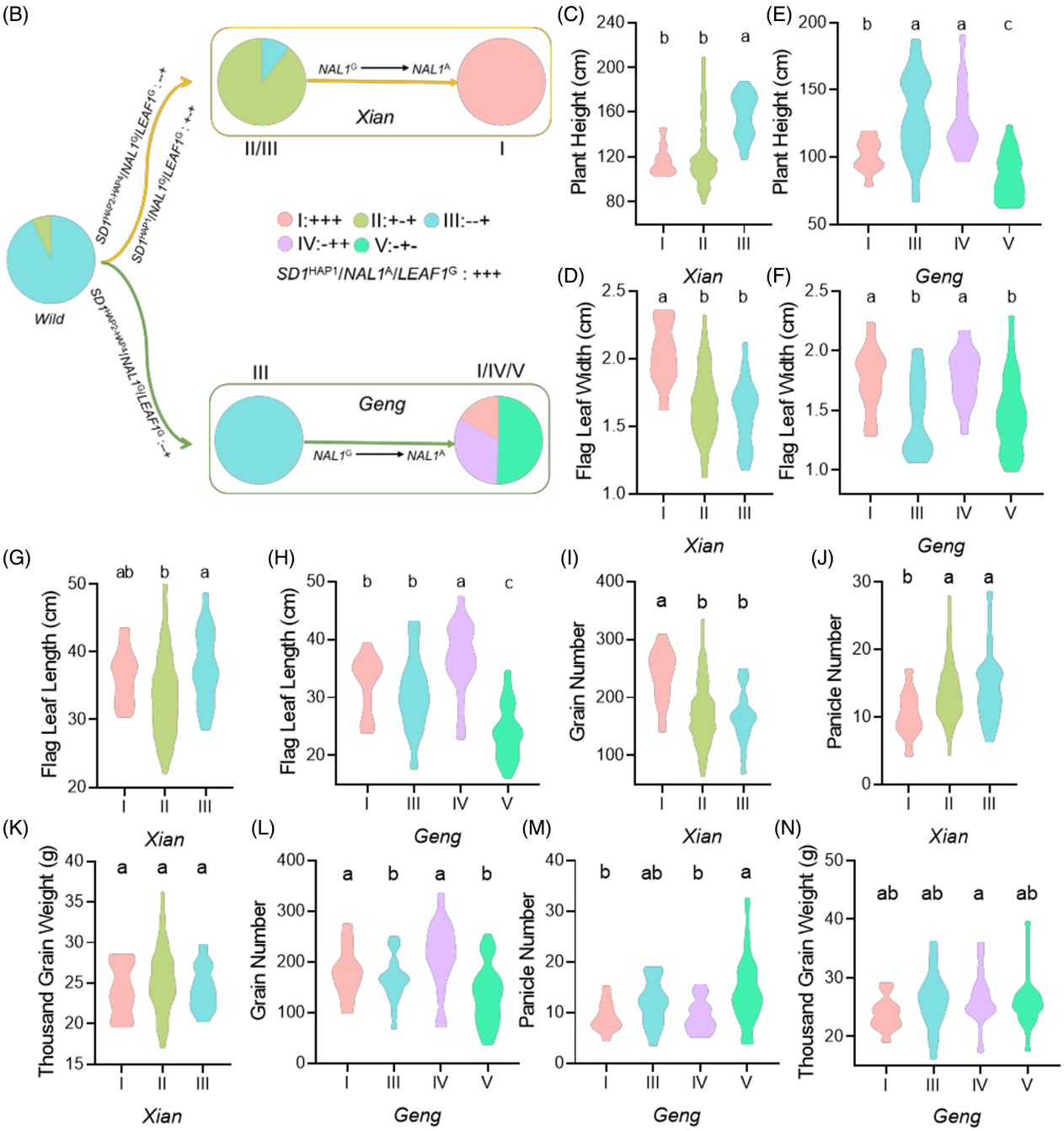

Figure 6. Pyramiding of *SD1*, *NAL1*, and *LEAF1* improves plant architecture and grain yield.
(A) Joint haplotype analysis of *SD1*, *NAL1*, and *LEAF1* in *Xian* and *Geng* subgroups. Data represent means ± SD ($n \geq 11$; $P < 0.05$; one-way ANOVA). The significance for the same lowercase letter is $P \geq 0.05$, while for the different lowercase letters are $P < 0.05$.
(B) Model of the breeding utilization of five main aggregation types.
(C–H) Differences in plant architecture among five main aggregation types in *Xian* and *Geng* subgroups, including plant height (C, E), flag leaf width (D, F), and flag leaf length (G, H). Data represent means ± SD ($n \geq 11$; $P < 0.05$; one-way ANOVA). The significance for the same lowercase letter is $P \geq 0.05$, while for the different lowercase letters are $P < 0.05$.
(I–N) Grain yield performance of five main aggregation types, including grain number (I, L), panicle number (J, M), and thousand grain weight (K, N). Data represent means ± SD ($n \geq 11$; $P < 0.05$; one-way ANOVA). The significance for the same lowercase letter is $P \geq 0.05$, while for the different lowercase letters are $P < 0.05$.

The genomic regions that have the potential to be co-selected for these three traits were identified. Previous studies mainly focused on a single trait, such as plant height or leaf morphology. The results from this study showed that there was a positive correlation between plant height and the leaf morphology traits (Table S2) and the positive correlation between plant height and flag leaf length was greatest; flag leaf length and width had a medium positive correlation, and plant height and flag leaf width had the lowest positive correlation. Among the loci identified by the GWAS, 13 loci associated with plant height and flag leaf length, 3 loci associated with plant height and flag leaf width, and 7 loci associated with flag leaf length and width were consistently detected (Figure 2C). However, no loci affecting plant height, flag leaf length, and flag leaf width were found, which might be due to a lower positive correlation between plant height and flag leaf width. Previous studies have shown that genomic differentiation and selection play critical roles in distinct morphological and physiological traits and the regional distribution of the different subspecies (Wang et al., 2022). Furthermore, *Xian* and *TrG* produced taller plants with increased leaf morphology traits, but lower coefficients of variation than those for *TeG* (Table S2; Figure S2). Numerous highly divergent genomic regions for the three traits were detected by the population differentiation statistics analysis (Figure 7A–C) and the differences among these genomic regions might be the underlying genetic basis for the plant morphology variations across subspecies. Among them, the proportion of highly divergent genomic regions that overlapped among the different traits between *Xian* or *TrG* and *TeG* was higher than intra-*TeG*. This indicated that the highly divergent genomic regions related to plant height, flag leaf length, and flag leaf width between *Xian* or *TrG* and *TeG* had a high degree of similarity; however, these regions varied considerably among the different *TeG* accessions. Moreover, the proportion of overlapping highly divergent genomic regions between plant height and flag leaf length was higher than that between flag leaf length and width (Table S20). Plant height and flag leaf width had the lowest proportion of overlapping highly divergent genomic regions (Table S20). A comparison between these highly divergent genomic regions and the loci identified by the GWAS showed that parts of these regions might contain genes that synergistically modulate different traits and that there might also be a convergence trend between these traits during the domestication process. The population genetics analysis revealed that *OsGH3-2* in *qPH1.10*/*qFLL1.33* and *LEAF1* in *qFLL8.1* might be co-domesticated genes for plant height and flag leaf length (Figure 7E–H). *OsGH3-2* overexpression lines have been shown to mimic the IAA deficiency phenotype, such as dwarfism and shorter flag leaves (Du et al., 2012). The *LEAF1* knockout lines in this study had lower plant heights and shorter flag leaves (Figure 4H–K; Figure S16) and some other cloned genes related to plant height, flag leaf length, and flag leaf width, such as *OsGA20ox1*, *OsXTH8*, *OsWAK10*, *OsXPO1*, *OFP1*, and *OsTZF1*, were located in these overlapping divergent regions (Tables S17–S19). These genes might be important regulatory genes for plant morphogenesis development.

In general, *Xian* tends to have relatively greater plant heights and longer or wider leaves (Figure S2). The production of sufficient biomass and photosynthates improves yield; however, excessive plant heights and large leaves increase lodging and shielding. *Geng* has strong lodging resistance due to its relatively lower plant height and shorter or narrower leaves (Figure S2). However, the lower biomass and photosynthate production reduce yield. The evolution and utilization of *SD1*, *NAL1*, and *LEAF1* in breeding were investigated to further understand how to select suitable genetic resources for improving plant aboveground morphology. All the *SD1* and *LEAF1* alleles and $NAL1^{G}$ had directly evolved from wild rice (Figure 5A; Figures S19A and S20A), but $NAL1^{A}$ was from a *de novo* mutation (Figure S20A). These natural alleles were retained in different improved varieties based on their different functions. For example, the dwarfing $SD1^{HAP1}$ allele could be utilized in *Xian* accessions with relatively high plant heights (Figure S19B), while the $SD1^{HAP2\text{-}HAP4}$ allele could be used in *Geng* with relatively low plant heights to maintain biomass and photosynthate production. The dominant wide flag leaf $NAL1^{A}$ allele has been mainly utilized in *Geng* with a relatively narrower flag leaf (Figure S20B), while the $NAL1^{G}$ allele could be used in *Xian* with a relatively wider flag leaf to maintain flat and upright leaves. Most of the improved *Xian* and *TrG* varieties contained the long flag leaf $LEAF1^{G}$ allele. This might be related to the function that *LEAF1* maintains the growth and

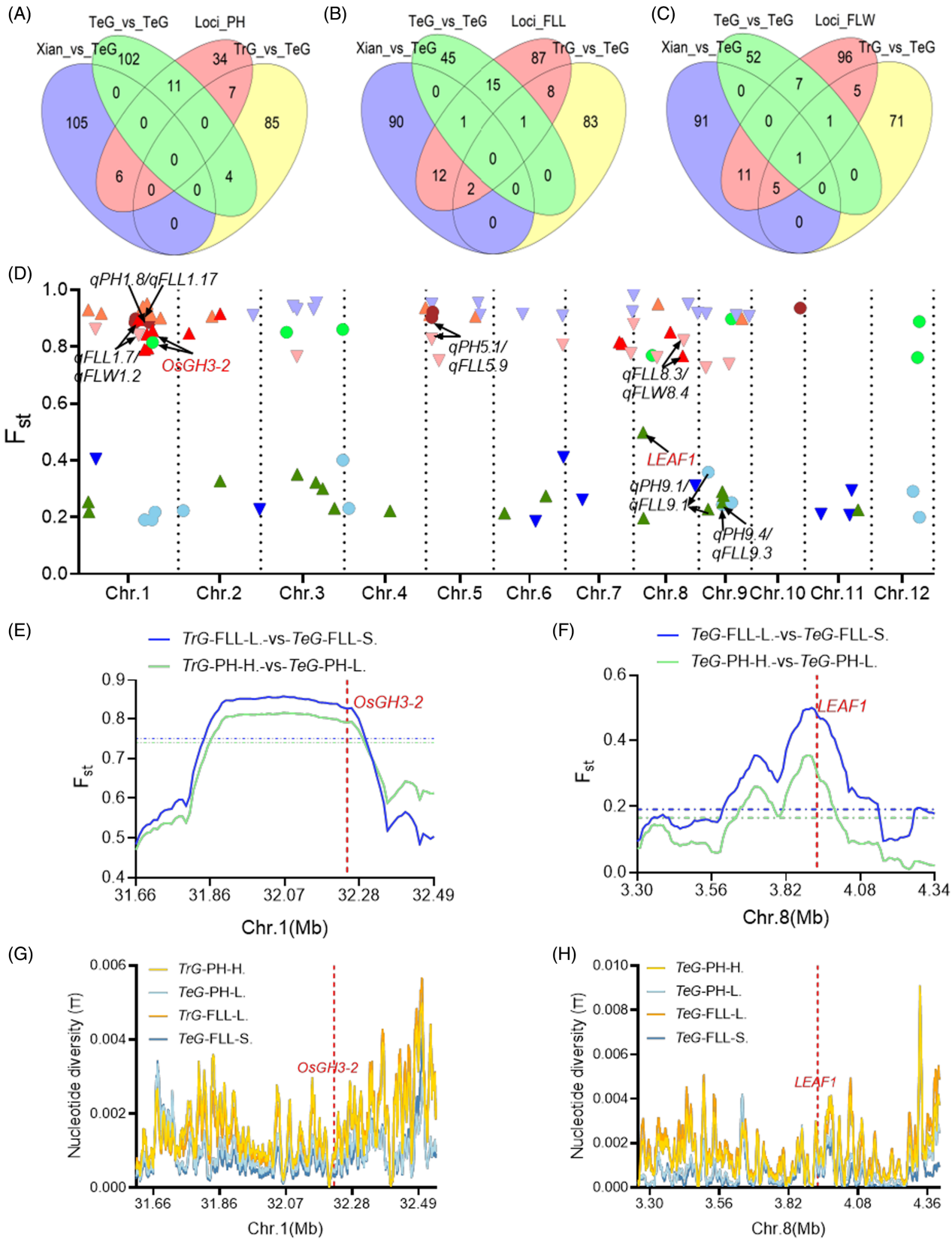

Figure 7. Uncovering genomic regions simultaneously regulating plant height and leaf morphology.
(A–C) Comparison of the divergent regions detected inter-subspecies and intra-*TeG* with loci associated with plant height (A), flag leaf length (B), and flag leaf width (C) through GWAS.
(D) Distribution of the highly overlapped divergent genomic regions associated with plant height, flag leaf length, and flag leaf width across 12 chromosomes. Overlapped loci from divergent regions are represented as follows: Brown circles, *Xian*-PH-H vs. *TeG*-PH-L; bright green circles, *TrG*-PH-H vs. *TeG*-PH-L; light blue circles, *TeG*-PH-H vs. *TeG*-PH-L; orange upper triangles, *Xian*-FLL-L vs. *TeG*-FLL-S; red upper triangles, *TrG*-FLL-L vs. *TeG*-FLL-S; dark green upper triangles, *TeG*-FLL-L vs. *TeG*-FLL-S; lavender lower triangles, *Xian*-FLW-W vs. *TeG*-FLW-N; pink lower triangles, *TrG*-FLW-W vs. *TeG*-FLW-N; dark blue lower triangles, *TeG*-FLW-W vs. *TeG*-FLW-N.
(E, F) Genetic differentiation of *OsGH3-2* (E) and *LEAF1* (F).
(G, H) The nucleotide diversity of *OsGH3-2* (G) and *LEAF1* (H) and their flank regions. Red vertical lines indicate the positions of *OsGH3-2* and *LEAF1*. *Xian/TrG/TeG*-PH-H., *Xian/TrG/TeG* with higher plant height; *TeG*-PH-L., *TeG* with lower plant height; *Xian/TrG/TeG*-FLL-L., *Xian/TrG/TeG* with longer flag leaf; *TeG*-FLL-S., *TeG* with shorter flag leaf; *Xian/TrG/TeG*-FLW-W., *Xian/TrG/TeG* with wider flag leaf; *TeG*-FLW-N., *TeG* with narrower flag leaf.

development of rice through its effects on cytokinin transport (Zhao et al., 2019). However, most *TeG* varieties contained the $LEAF1^{A}$ allele, which might be associated with dwarfing breeding.

The joint haplotype analysis of three genes suggested that different combinations of the alleles could provide abundant genetic resources for ideal plant height and flag leaf breeding (Figure 6A). The only difference between Type II and Type III plants was the *SD1* allele. In *Xian*, the Type II plants, which carried the $SD1^{HAP1}$ allele, had lower plant heights and shorter flag leaves compared with Type III, which did not have the $SD1^{HAP1}$ allele (Figure 6C,G). Similarly, in the *Geng* accessions, the Type I plants, which contained the $SD1^{HAP1}$ allele, had lower plant heights and shorter flag leaves relative to Type IV, which lacks the $SD1^{HAP1}$ allele (Figure 6E,H). Previous studies have shown that *SD1* encodes the biosynthesis enzyme GA20ox-2, which was strongly expressed in the leaf blade and stem, and that the enzyme-defective *sd1* mutants had shorter leaves and stems (Sasaki et al., 2002). These results indicated that *SD1* might also have a functional role in leaf morphology. Although Types I and II had lower plant heights and shorter flag leaves, their yield-related traits were comparable to those of Types III and IV (Figure 6I–N). Thus, pyramiding favorable alleles of different genes could effectively improve multiple traits, and selecting appropriate allele combinations will help achieve customized breeding goals. Therefore, it is important to understand the characteristics of the materials themselves and to consider the relationship between plant height and leaf shape when attempting to improve plant aboveground morphology. This information could improve the selection of suitable genetic resources for effective improvement.

LEAF1 was a pleiotropic gene. Knockout lines of *LEAF1* had shorter and narrower flag leaves, lower plant heights, thinner stems, shorter panicle lengths, decreased primary and secondary branches, and reduced grain numbers (Figure 4H–K; Figure S16). However, the introgression line IL81 contained segments from *TrG* accession IRAT109 with the $LEAF1^{G}$ allele in the background of the *TeG* accession Yuefu, which contains the $LEAF1^{A}$ allele. This line had longer flag leaves and greater plant heights (Figure 5E–H). These results indicated that the $LEAF1^{G}$ allele could be used to improve leaf architecture in *TeG*. *LEAF1* is essential for the long-distance transport of root-derived cytokinins (Zhao et al., 2019). We speculated that the transport of root-derived cytokinins was significantly suppressed in the *LEAF1* knockout lines. The growth and development of aboveground leaves, stems, and other source organs were inhibited due to the lack of cytokinins, leading to the decreased accumulation of carbohydrates at the vegetative growth stage. When the plant changed from vegetative growth to reproductive growth, the carbohydrates released by source organs, such as flag leaves, through photosynthesis could not create an adequate total sink storage capacity and tended to form a panicle morphology that reduced grain numbers but increased grain size. This suggested that *LEAF1* could modulate the source-sink balance by maintaining the transport of root-derived cytokinins to the aboveground organs. However, this needs to be confirmed by future studies.

MATERIALS AND METHODS

Plant materials and growth conditions

A total of 689 cultivated rice accessions from 41 countries and regions, including 452 *Xian* and 237 *Geng* (200 temperate *Geng* and 37 tropical *Geng*) were used in this study. Among them, 655 accessions were planted in Nanning, Guangxi Zhuang Autonomous Region, in 2020, and 396 accessions were planted in Beijing in 2021 with two duplicates, respectively. The detailed information of these accessions was listed in Table S1.

Phenotyping

At the grain filling stage, the plant height, flag leaf length, and flag leaf width corresponding to the highest three panicles were selected to be artificially phenotyped. Plant height is defined as the distance from the ground to the top of the panicle. Flag leaf length measures the distance from the pillow to the tip of the leaf in a flat position. Flag leaf width measures the distance between the left and right edges of the broadest blade in flat. R packages "PerformanceAnalytics" was used to perform correlation analysis.

Population structure analysis

Sequencing data were available from the 3000 Rice Genome Project (3KRGP) with an average sequencing depth of 15× (Wang et al., 2018). 305 998 SNPs evenly distributed throughout the genome were screened and were used to construct a neighbor-joining tree in MEGA version 7 with the bootstrap method and 1000 replicates (Kumar et al., 2016). The genome-wide LD decay of the association

populations was determined using PopLDdecay version 3.4 with parameters as follows: -maxdist 5000; -maf 0.05; -miss 0.25 (Zhang et al., 2019). The LD decay distance was determined as the LD decays to half of the maximum value (Zhao et al., 2018).

GWAS

A total of 3 059 978 high-quality SNPs (MAF ≥5%, missing rate <25%) were used to perform GWAS using both the general linear model and compressed mixed linear model in the GAPIT package operated in an R environment (Tang et al., 2016). The population structure of PCA and kinship was a cofactor when performing GWAS using the CMLM model. The genome-wide significance threshold was determined by permutation tests with 1000 replications (Zhao et al., 2018). A region with more than three consecutive significant SNPs and the distance between two SNPs less than LD decay distance was considered a single significant associated signal (Guo et al., 2020). The SNP with the minimum *P*-value within the significant associated signal was designated as the lead-SNP. For the analysis of candidate genes of the significant associated signal, the continuous region containing SNPs closely linked with each other ($r^2 \geq 0.6$) was considered the local LD interval (Yano et al., 2016).

Population genetics analysis

To clarify the differentiation and selection of plant height, flag leaf length, and flag leaf width, the population differentiation statistics (F_{ST}), nucleotide diversity (π), and Tajima's *D* were calculated by using VCFtools software (Danecek et al., 2011). F_{ST} and nucleotide diversity were computed using 100-kb windows and 10-kb steps, and Tajima's *D* was calculated using 10-kb windows. Sliding windows with the top 5% of F_{ST} values were identified as divergent windows. Regions with average Tajima's $D < -1$ and Tajima's $D > 1$ might be under directional or balanced selection (Qiu et al., 2017; Xia et al., 2019). Tajima's *D* of the gene and its 100 kb flanking region were estimated by DnaSP 5.10 (Librado & Rozas, 2009).

Haplotype analysis

The haplotypes of candidate genes were constructed based on SNPs in a 2 kb promoter and non-synonymous SNPs in the coding region. Plant height, flag leaf length, or flag leaf width of cultivated rice accessions in GWAS were used to make multiple comparisons of phenotypes. The haplotypes contain more than five or ten rice accessions that were retained for single gene or joint haplotype analysis.

Evolutionary analysis

A minimum spanning tree among haplotypes was calculated using Arlequin version 3.5 (Excoffier & Lischer, 2010) and drawn in Hapstar-0.7 (Teacher & Griffiths, 2011).

Plasmid construction and rice transformation

To construct the CRISPR/Cas9 vector, two 20 bp targets from the coding sequence of *LEAF1* were designed, respectively, for specific recognition and cloned into the vector pHUE411, as previously described (Xing et al., 2014). The coding sequence of *LEAF1* without the stop codon from the "Huanghuazhan" (HAP1) accession was integrated into pSuper1300-MYC to construct the *LEAF1* complementary vector. To produce transgenic plants, the corresponding constructs were introduced into Agrobacterium tumefaciens strain *EHA105* and subsequently transformed into rice calli from mature embryos via *Agrobacterium*-mediated transformation (Hiei et al., 1994; Toki et al., 2006).

qRT-PCR

Total RNA was extracted from leaf tissues using the RNApure Total RNA Kit (Aidlab, Beijing, China) following the manufacturer's protocol. The full-length cDNA was reverse transcribed using HiScript II Reverse Transcriptase (Vazyme, Nanjing, China) according to the manufacturer's instructions. Quantitative PCR (qPCR) was carried out using the TB Green Premix Ex Taq II (TaKaRa, Kyoto, Japan) as previously described (Zhang, Li, et al., 2017). The *OsACTIN* gene was used as an internal control for normalization (Livak & Schmittgen, 2001).

Primers

The relevant primers used are listed in Table S21.

AUTHOR CONTRIBUTIONS

XW, ZLi, and ZZ designed the research. ZZ, NJ, XQ, XZ, RL, QH, and XW contributed to the phenotyping of rice germplasm. LC, ZLiu, and XW performed transgenic validations of causal genes. NJ, XZ, and XW analyzed the data. LC, DL, PX, XS, JL, and HZ performed part of the experiments. YP, ZLi, and ZZ conceived and supervised the project. NUK, ZZ, ZLi, and XW wrote the manuscript.

ACKNOWLEDGEMENTS

This work was supported by Biological Breeding-National Science and Technology Major Project (2023ZD0406803), the National Natural Science Foundation of China (32272123 and 32072036), the Chinese Universities Scientific Fund (2024TC189), the open project of Guangxi Academy of Agricultural Sciences (2022-36-Z01-KF03) and the Special Plan for Key Laboratory of "Western Light Western cross team" (xbzg-zdsys-202111).

CONFLICT OF INTEREST

The authors declare no conflict of interest.

DATA AVAILABILITY STATEMENT

All relevant data can be found within the manuscript and its supporting materials.

SUPPORTING INFORMATION

Additional Supporting Information may be found in the online version of this article.

Figure S1. Phenotypic characterization of rice germplasm in 2021.

Figure S2. Phenotypic analysis of different rice subspecies in 2020 and 2021.

Figure S3. Neighbor-joining tree and principal component analyses of rice germplasms.

Figure S4. LD decay of the total germplasms, *Xian*, and *Geng* in 2020 and 2021.

Figure S5. Quantile-quantile plots for the general linear model (GLM).

Figure S6. Quantile-quantile plots for the compressed mixed linear model (CMLM).

Figure S7. Genome-wide threshold for GWAS based on the permutation tests.

Figure S8. GWAS for plant height in the total germplasm, *Xian*, and *Geng* in 2020.

Figure S9. GWAS for flag leaf width in the total germplasm, *Xian*, and *Geng* in 2020 and 2021.

Figure S10. GWAS for flag leaf length in the total germplasm, *Xian* and *Geng* in 2020 and 2021.

Figure S11. Analysis of identified co-loci.

Figure S12. The flag leaf width among haplotypes of *NAL1*.

Figure S13. Candidate gene analysis of *qFLL8.1*.

Figure S14. Expression levels and homology analysis of *LEAF1*.

Figure S15. Analysis of candidate gene *LEAF1* identified by GWAS.

Figure S16. Agronomic traits identification of the knockout lines *leaf1*-1 and *leaf1*-2.

Figure S17. The plant height among haplotypes of *LEAF1*.

Figure S18. Functional validation of *LEAF1*^{G}-complementary lines.

Figure S19. Evolution and breeding analysis of *SD1*.

Figure S20. Evolution and breeding analysis of *NAL1*.

Figure S21. Genomic differentiation of plant height, flag leaf length, and flag leaf width between *Xian* and *TeG*.

Figure S22. Genomic differentiation of plant height, flag leaf length, and flag leaf width between *TrG* and *TeG*.

Figure S23. Genomic differentiation of plant height, flag leaf length, and flag leaf width intra-*TeG*.

Figure S24. Average nucleotide diversity of genomic and divergent regions inter-subspecies and intra-*TeG*.

Table S1. Information of *Oryza sativa* L. varieties and wild rice.

Table S2. Statistics of plant height, flag leaf length, and flag leaf width in 2020 and 2021 used in this study.

Table S3. Correlation analysis of plant height, flag leaf length, and flag leaf width in 2020 and 2021.

Table S4. Information of the loci associated with plant height, flag leaf length, and flag leaf width identified by GWAS of different association populations in 2020 and 2021.

Table S5. Haplotype analysis of candidate genes.

Table S6. Estimates of nucleotide diversity and Tajima's *D* value of genes and their flanking region.

Table S7. Field traits of different alleles of three genes between landraces and improved varieties.

Table S8. Genomic regions differentiated between *Xian*-PH-H and *TeG*-PH-L.

Table S9. Genomic regions differentiated between *TrG*-PH-H and *TeG*-PH-L.

Table S10. Genomic regions differentiated between *TeG*-PH-H and *TeG*-PH-L.

Table S11. Genomic regions differentiated between *Xian*-FLL-L and *TeG*-FLL-S.

Table S12. Genomic regions differentiated between *TrG*-FLL-L and *TeG*-FLL-S.

Table S13. Genomic regions differentiated between *TeG*-FLL-L and *TeG*-FLL-S.

Table S14. Genomic regions differentiated between *Xian*-FLW-W and *TeG*-FLW-N.

Table S15. Genomic regions differentiated between *TrG*-FLW-W and *TeG*-FLW-N.

Table S16. Genomic regions differentiated between *TeG*-FLW-W and *TeG*-FLW-N.

Table S17. Population genetic parameters of highly divergent overlapped region of plant height.

Table S18. Population genetic parameters of highly divergent overlapped region of flag leaf length.

Table S19. Population genetic parameters of highly divergent overlapped region of flag leaf width.

Table S20. Divergent overlapped region detected from three groups among plant height, flag leaf length and flag leaf width.

Table S21. Primers used in this study.

REFERENCES

Acevedo-Siaca, L., Coe, R., Quick, W. & Long, S. (2021) Variation between rice accessions in photosynthetic induction in flag leaves and underlying mechanisms. *Journal of Experimental Botany*, **72**(4), 1282–1294.

Adachi, S., Yoshikawa, K., Yamanouchi, U., Tanabata, T., Sun, J., Ookawa, T. *et al.* (2017) Fine mapping of *Carbon Assimilation Rate 8*, a quantitative trait locus for flag leaf nitrogen content, stomatal conductance and photosynthesis in rice. *Frontiers in Plant Science*, **8**(60), 60. Available from: https://doi.org/10.3389/fpls.2017.00060

Cai, W., Hong, J., Liu, Z., Wang, W., Zhang, J., An, G. *et al.* (2023) A receptor-like kinase controls the amplitude of secondary cell wall synthesis in rice. *Current Biology*, **33**, 498–506.

Chen, J., Tang, W., Hong, M. & Wang, Z. (2003) *OsBP-73*, a rice gene, encodes a novel DNA-binding protein with a SAP-like domain and its genetic interference by double-stranded RNA inhibits rice growth. *Plant Molecular Biology*, **52**, 579–590.

Chen, K., Guo, T., Li, X., Yang, Y., Dong, N., Shi, C. *et al.* (2019) *NAL8* encodes a prohibitin that contributes to leaf and spikelet development by regulating mitochondria and chloroplasts stability in rice. *BMC Plant Biology*, **19**, 395.

Danecek, P., Auton, A., Abecasis, G., Albers, C., Banks, E., DePristo, M. *et al.* (2011) The variant call format and VCFtools. *Bioinformatics*, **27**, 2156–2158.

Du, H., Wu, N., Fu, J., Wang, S., Li, X., Xiao, J. *et al.* (2012) A *GH3* family member, *OsGH3-2*, modulates auxin and abscisic acid levels and differentially affects drought and cold tolerance in rice. *Journal of Experimental Botany*, **63**(18), 6467–6480.

Excoffier, L. & Lischer, H. (2010) Arlequin suite ver 3.5: a new series of programs to perform population genetics analyses under Linux and Windows. *Molecular Ecology Resources*, **10**, 564–567.

Guo, H., Zeng, Y., Li, J., Ma, X., Zhang, Z., Lou, Q. *et al.* (2020) Differentiation, evolution and utilization of natural alleles for cold adaptability at the reproductive stage in rice. *Plant Biotechnology Journal*, **18**, 2491–2503.

He, P., Wang, X., Zhang, X., Jiang, Y., Tian, W., Zhang, X. *et al.* (2018) Short and narrow flag leaf1, a GATA zinc finger domain-containing protein, regulates flag leaf size in rice (*Oryza sativa* L.). *BMC Plant Biology*, **18**, 273.

Hiei, Y., Ohta, S., Komari, T. & Kumashiro, T. (1994) Efficient transformation of rice (*Oryza sativa* L.) mediated by Agrobacterium and sequence analysis of the boundaries of the T-DNA. *The Plant Journal*, **6**, 271–282.

Hong, Z., Ueguchi-Tanaka, M., Umemura, K., Uozu, S., Fujioka, S., Takatsuto, S. *et al.* (2003) A Rice brassinosteroid-deficient mutant, *ebisu dwarf* (*d2*), is caused by a loss of function of a new member of cytochrome P450. *The Plant Cell*, **15**(12), 2900–2910.

Huang, X., Kurata, N., Wei, X., Wang, Z., Wang, A., Zhao, Q. *et al.* (2012) A map of rice genome variation reveals the origin of cultivated rice. *Nature*, **490**, 497–501.

Itoh, H., Tatsumi, T., Sakamoto, T., Otomo, K., Toyomasu, T., Kitano, H. *et al.* (2004) A rice semi-dwarf gene, *Tan-Ginbozu* (*D35*), nncodes the gibberellin biosynthesis enzyme, ent-kaurene oxidase. *Plant Molecular Biology*, **54**(4), 533–547.

Jan, A., Yang, G., Nakamura, H., Ichikawa, H., Kitano, H., Matsuoka, M. *et al.* (2004) Characterization of a xyloglucan endotransglucosylase gene that is up-regulated by gibberellin in rice. *Plant Physiology*, **136**, 3670–3681.

Jiao, Y., Wang, Y., Xue, D., Wang, J., Yan, M., Liu, G. *et al.* (2010) Regulation of *OsSPL14* by *OsmiR156* defines ideal plant architecture in rice. *Nature Genetics*, **42**(6), 541–544. Available from: https://doi.org/10.1038/ng.591

Jing, C., Zhang, F., Wang, X., Wang, M., Lian Zhou, L., Cai, Z. *et al.* (2023) Multiple domestications of Asian rice. *Nature Plants*, **9**, 1221–1235.

Ko, D., **Kang, J.**, **Kiba, T.** & **Lee, Y.** (2014) Arabidopsis *ABCG14* is essential for the root-to-shoot translocation of cytokinin. *Proceedings of the National Academy of Sciences*, **111**(19), 7150–7155.

Kumar, S., **Stecher, G.** & **Tamura, K.** (2016) MEGA7: molecular evolutionary genetics analysis version 7.0 for bigger datasets. *Molecular Biology and Evolution*, **33**, 1870–1874.

Lee, J., **Moon, S.**, **Jang, S.**, **Lee, S.**, **An, G.**, **Jung, K.** ***et al.*** (2020) *OsbHLH073* negatively regulates internode elongation and plant height by modulating GA homeostasis in rice. *Plants*, **9**, 547.

Li, W., **Wu, C.**, **Hu, G.**, **Xing, L.**, **Qian, W.**, **Si, H.** ***et al.*** (2013) Characterization and fine mapping of a novel rice narrow leaf mutant *nal9*. *Journal of Integrative Plant Biology*, **55**(11), 1016–1025.

Librado, P. & **Rozas, J.** (2009) DnaSP v5: a software for comprehensive analysis of DNA polymorphism data. *Bioinformatics*, **25**, 1451–1452.

Liu, Q., **Wu, K.**, **Harberd, N.** & **Fu, X.** (2021) Green revolution DELLAs: from translational reinitiation to future sustainable agriculture. *Molecular Plant*, **14**, 547–549.

Livak, K.J. & **Schmittgen, T.D.** (2001) Analysis of relative gene expression data using real-time quantitative PCR and the $2^{-\Delta\Delta CT}$ method. *Methods*, **25**, 402–408.

Lu, Y., **Meng, Y.**, **Zeng, J.**, **Luo, Y.**, **Feng, Z.**, **Bian, Y.** ***et al.*** (2020) Coordination between *GROWTH-REGULATING FACTOR1* and *GRF-INTERACTING FACTOR1* plays a key role in regulating leaf growth in rice. *BMC Plant Biology*, **20**, 200.

Oikawa, T., **Koshioka, M.**, **Kojima, K.**, **Yoshida, H.** & **Kawata, M.** (2004) A role of *OsGA20ox1*, encoding an isoform of gibberellin 20-oxidase, for regulation of plant stature in rice. *Plant Molecular Biology*, **55**, 687–700.

Peng, Q., **Qiu, J.**, **Li, X.**, **Xu, X.**, **Peng, X.** & **Zhu, G.** (2023) The nuclear export receptor *OsXPO1* is required for rice development and involved in abiotic stress responses. *The Crop Journal*, **11**, 71–78.

Qi, J., **Qian, Q.**, **Bu, Q.**, **Li, S.**, **Chen, Q.**, **Sun, J.** ***et al.*** (2008) Mutation of the rice *narrow leaf1* gene, which encodes a novel protein, affects vein patterning and polar auxin transport. *Plant Physiology*, **147**, 1947–1959.

Qiu, J., **Zhou, Y.**, **Mao, L.**, **Ye, C.**, **Wang, W.**, **Zhang, J.** ***et al.*** (2017) Genomic variation associated with local adaptation of weedy rice during de-domestication. *Nature Communications*, **8**(1), 15323. Available from: https://doi.org/10.1038/ncomms15323

Qu, M., **Zheng, G.**, **Hamdani, S.**, **Essemine, J.**, **Song, Q.**, **Wang, H.** ***et al.*** (2017) Leaf photosynthetic parameters related to biomass accumulation in a global rice diversity survey. *Plant Physiology*, **175**(1), 248–258. Available from: https://doi.org/10.1104/pp.17.00332

Rahman, M., **Haque, M.**, **Sikdar, B.**, **Islam, M.** & **Matin, M.** (2013) Correlation analysis of flag leaf with yield in several rice cultivars. *Journal Life Earth Science*, **8**, 49–54.

Rong, C., **Liu, Y.**, **Chang, Z.**, **Liu, Z.**, **Ding, Y.** & **Ding, C.** (2022) Cytokinin oxidase/dehydrogenase family genes exhibit functional divergence and overlap in rice growth and development, especially in control of tillering. *Journal of Experimental Botany*, **73**(11), 3552–3568.

Sasaki, A., **Ashikari, M.**, **Ueguchi-Tanaka, M.**, **Itoh, H.**, **Nishimura, A.**, **Swapan, D.** ***et al.*** (2002) A mutant gibberellin-synthesis gene in rice. *Nature*, **416**, 701–702.

Tanabe, S., **Ashikari, M.**, **Fujioka, S.**, **Takatsuto, S.**, **Yoshida, S.**, **Yano, M.** ***et al.*** (2005) A novel cytochrome P450 is implicated in brassinosteroid biosynthesis via the characterization of a rice dwarf mutant, *dwarf11*, with reduced seed length. *The Plant Cell*, **17**(3), 776–790.

Tang, Y., **Liu, X.**, **Wang, J.**, **Li, M.**, **Wang, Q.**, **Tian, F.** ***et al.*** (2016) GAPIT version 2: an enhanced integrated tool for genomic association and prediction. *Plant Genome*, **9**(2), 1–9.

Teacher, A. & **Griffiths, D.** (2011) HapStar: automated haplotype network layout and visualization. *Molecular Ecology Resources*, **11**, 151–153.

Toki, S., **Hara, N.**, **Ono, K.**, **Onodera, H.**, **Tagiri, A.**, **Oka, S.** ***et al.*** (2006) Early infection of scutellum tissue with Agrobacterium allows high-speed transformation of rice. *The Plant Journal*, **47**, 969–976.

Ueguchi-Tanaka, M., **Fujisawa, Y.**, **Kobayashi, M.**, **Ashikari, M.**, **Iwasaki, Y.**, **Kitano, H.** ***et al.*** (2000) Rice dwarf mutant *d1*, which is defective in the α subunit of the heterotrimeric G protein, affects gibberellin signal transduction. *Proceedings of the National Academy of Sciences*, **97**(21), 11638–11643.

Uzaira, M., **Long, H.**, **Zafar, S.**, **Patil, S.**, **Chun, Y.**, **Li, L.** ***et al.*** (2021) *Narrow Leaf 21*, encoding ribosomal protein RPS3A, controls leaf development in Rice. *Plant Physiology*, **186**(1), 497–518.

Wang, C., **Yu, H.**, **Huang, J.**, **Wang, W.**, **Faruquee, M.**, **Zhang, F.** ***et al.*** (2020) Towards a deeper haplotype mining of complex traits in rice with RFGB v2.0. *Plant Biotechnology Journal*, **18**(1), 14–16. Available from: https://doi.org/10.1111/pbi.13215

Wang, J., **Wang, T.**, **Wang, Q.**, **Tang, X.**, **Ren, Y.**, **Zheng, H.** ***et al.*** (2022) QTL mapping and candidate gene mining of fag leaf size traits in Japonica rice based on linkage mapping and genome-wide association study. *Molecular Biology Reports*, **49**, 63–71.

Wang, M., **Huang, L.**, **Kou, Y.**, **Li, D.**, **Hu, W.**, **Fan, D.** ***et al.*** (2023) Differentiation of morphological traits and genome-wide expression patterns between rice subspecies *indica* and *japonica*. *Genes*, **14**, 1971.

Wang, W., **Mauleon, R.**, **Hu, Z.**, **Chebotarov, D.**, **Tai, S.**, **Wu, Z.** ***et al.*** (2018) Genomic variation in 3,010 diverse accessions of Asian cultivated rice. *Nature*, **557**, 43–49.

Xia, H., **Luo, Z.**, **Xiong, J.**, **Ma, X.**, **Lou, Q.**, **Wei, H.** ***et al.*** (2019) Bi-directional selection in upland rice leads to its adaptive differentiation from lowland rice in drought resistance and productivity. *Molecular Plant*, **12**, 170–184.

Xiao, Y., **Liu, D.**, **Zhang, G.**, **Tong, H.** & **Chu, C.** (2017) Brassinosteroids regulate OFP1, a DLT interacting protein, to modulate plant architecture and grain morphology in rice. *Frontiers in Plant Science*, **8**(1698), 1698. Available from: https://doi.org/10.3389/fpls.2017.01698

Xing, H., **Dong, L.**, **Wang, Z.**, **Zhang, H.**, **Han, C.**, **Liu, B.** ***et al.*** (2014) A CRISPR/Cas9 toolkit for multiplex genome editing in plants. *BMC Plant Biology*, **14**, 327.

Xu, J., **Shang, L.**, **Wang, J.**, **Chen, M.**, **Fu, X.**, **He, H.** ***et al.*** (2021) The *SEEDLING BIOMASS 1* allele from indica rice enhances yield performance under low-nitrogen environments. *Plant Biotechnology Journal*, **19**, 1681–1683.

Yano, K., **Yamamoto, E.**, **Aya, K.**, **Takeuchi, H.**, **Lo, P.**, **Hu, L.** ***et al.*** (2016) Genome-wide association study using whole-genome sequencing rapidly identifies new genes influencing agronomic traits in rice. *Nature Genetics*, **48**, 927–934.

You, J., **Xiao, W.**, **Zhou, Y.**, **Shen, W.**, **Ye, L.**, **Yu, P.** ***et al.*** (2022) The APC/C^{TAD1} -WIDE LEAF 1-NARROW LEAF 1 pathway controls leaf width in rice. *The Plant Cell*, **34**, 4313–4328.

Zhang, C., **Dong, S.**, **Xu, J.**, **He, W.** & **Yang, T.** (2019) PopLDdecay: a fast and effective tool for linkage disequilibrium decay analysis based on variant call format files. *Bioinformatics*, **35**, 1786–1788.

Zhang, C., **Fang Zhang, F.**, **Zhou, J.**, **Fan, Z.**, **Chen, F.**, **Ma, H.** ***et al.*** (2012) Overexpression of a phytochrome-regulated tandem zinc finger protein gene, *OsTZF1*, confers hypersensitivity to ABA and hyposensitivity to red light and far-red light in rice seedlings. *Plant Cell Reports*, **31**, 1333–1343.

Zhang, Y., **Zhou, L.**, **Shen, X.**, **Chen, D.**, **Wu, W.**, **Zhan, X.** ***et al.*** (2017) Genetic dissection of yield traits in super hybrid rice Xieyou9308 using both unconditional and conditional genome-wide association mapping. *Scientific Reports*, **7**, 824.

Zhang, Z., **Li, J.**, **Pan, Y.**, **Li, J.**, **Zhou, L.**, **Shi, H.** ***et al.*** (2017) Natural variation in *CTB4a* enhances rice adaptation to cold habitats. *Nature Communications*, **8**, 14788.

Zhao, J., **Yu, N.**, **Ju, M.**, **Fan, B.**, **Zhang, Y.**, **Zhu, E.** ***et al.*** (2019) ABC transporter OsABCG18 controls the shootward transport of cytokinins and grain yield in rice. *Journal of Experimental Botany*, **70**(21), 6277–6291.

Zhao, Y., **Zhang, H.**, **Xu, J.**, **Jiang, C.**, **Yin, Z.**, **Xiong, H.** ***et al.*** (2018) Loci and natural alleles underlying robust roots and adaptive domestication of upland ecotype rice in aerobic conditions. *PLoS Genetics*, **14**, e1007521.

Zheng, T., **Yu, H.**, **Zhang, H.**, **Wu, Z.**, **Wang, W.**, **Tai, S.** ***et al.*** (2015) Rice functional genomics and breeding database (RFGB)-3K-rice SNP and InDel sub-database. *Chinese Science Bulletin*, **60**, 367–371.